Received: 29 August 2019 | Revised: 6 April 2020 | Accepted: 19 April 2020

DOI: 10.1002/eco.2213

WILEY

RESEARCH ARTICLE

Root-zone soil moisture variability across African savannas: From pulsed rainfall to land-cover switches

Matti Räsänen[1] | Lutz Merbold[2] | Ville Vakkari[3,4] | Mika Aurela[3] | Lauri Laakso[4,5] | J. Paul Beukes[4] | Pieter G. Van Zyl[4] | Miroslav Josipovic[4] | Gregor Feig[6,7] | Petri Pellikka[1,8] | Janne Rinne[9] | Gabriel G. Katul[10]

[1]Institute for Atmospheric and Earth System Research, University of Helsinki, Helsinki, Finland

[2]Mazingira Centre, International Livestock Research Institute, Nairobi, Kenya

[3]Climate Research Program, Finnish Meteorological Institute, Helsinki, Finland

[4]Atmospheric Chemistry Research Group, Chemical Resource Beneficiation, North-West University, Potchefstroom, South Africa

[5]Meteorological and Marine Research Program, Finnish Meteorological Institute, Helsinki, Finland

[6]Natural Resources and the Environment, Council for Scientific and Industrial Research, Pretoria, South Africa

[7]Department of Geography Geoinformatics and Meteorology, University of Pretoria, Pretoria, South Africa

[8]Department of Geosciences and Geography, University of Helsinki, Helsinki, Finland

[9]Department of Physical Geography and Ecosystem Science, Lund University, Lund, Sweden

[10]Nicholas School of the Environment, Duke University, Durham, NC, USA

Correspondence
Matti Räsänen, Institute for Atmospheric and Earth System Research, University of Helsinki, Helsinki, Finland.
Email: matti.rasanen@helsinki.fi

Funding information
National Science Foundation, Grant/Award Numbers: NSF-AGS-1644382, NSF-EAR-1344703, NSF-IOS-1754893; European Commission, Grant/Award Number: 730995; Bundesministerium für Bildung und Forschung, Grant/Award Number: 01LL1303; Academy of Finland,Grant/AwardNumbers:261280,318645

Abstract

The main source of soil moisture variability in savanna ecosystems is pulsed rainfall. Rainfall pulsing impacts water-stress durations, soil moisture switching between wet-to-dry and dry-to-wet states, and soil moisture spectra as well as derived measures from it such as soil moisture memory. Rainfall pulsing is also responsible for rapid changes in grassland leaf area and concomitant changes in evapotranspirational (ET) losses, which then impact soil moisture variability. With the use of a hierarchy of models and soil moisture measurements, temporal variability in root-zone soil moisture and water-stress periods are analysed at four African sites ranging from grass to miombo savannas. The normalized difference vegetation index (NDVI) and potential ET (PET)-adjusted ET model predict memory timescale and dry persistence in agreement with measurements. The model comparisons demonstrate that dry persistence and mean annual dry periods must account for seasonal and interannual changes in maximum ET represented by NDVI and to a lesser extent PET. Interestingly, the precipitation intensity and soil moisture memory were linearly related across three savannas with ET/infiltration $\sim$ 1.0. This relation and the variability of length and timing of dry periods are also discussed.

KEYWORDS

memory, persistence, precipitation intensity, savanna

1 | INTRODUCTION

In savanna ecosystems, sparsely spaced woody vegetation allows ample photosynthetically active radiation (PAR) to reach the ground surface, thereby promoting a herbaceous layer (primarily grasses) to compete for water with the woody vegetation. Because PAR rarely restricts the overall productivity of savannas, the carbon–water economies in such ecosystems are driven by rainfall pulses (Schwinning & Sala, 2004; Williams & Albertson, 2004) resulting in high temporal variability in root-zone soil moisture. Because the interpulse period and precipitation depth per event are random (at least on daily timescales), the surface soil moisture variability has been presumed to be primarily driven by stochastic rainfall events adjusted by interception and losses from the root zone due to drainage, root-water uptake and surface evaporation (Laio, Porporato, Fernandez-Illescas, & Rodriguez-Iturbe, 2001; Miller, Baldocchi, Law, & Meyers, 2007; Yin, Porporato, & Albertson, 2014). Soil moisture variability has also been shown to exert control on drought occurrence (Masih, Maskey, Mussá, & Trambauer, 2014; Saini, Wang, & Pal, 2016), probabilistic drought prediction (AghaKouchak, 2015), convective rainfall formation (Green et al., 2017; Koster et al., 2004; Siqueira, Katul, & Porporato, 2009; Taylor et al., 2011; Wei, Dickinson, & Chen, 2008) and ecosystem resilience (Porporato, Daly, & Rodriguez-Iturbe, 2004) primarily because soil moisture memory and persistence within certain phases (wet or dry) exceed the timescale of many meteorological variables. Such meteorological variables can then 'feed-off' on the soil moisture state of savanna ecosystems and be altered in a manner to impact rainfall occurrences and depth. The soil moisture variability is also related to phenology and root-water uptake that are not well represented in terrestrial biosphere models (Whitley et al., 2016; Whitley et al., 2017). For these reasons, the controls on soil moisture memory and dry persistence experienced by African savannas are receiving renewed interest, especially in climate studies (Ghannam et al., 2016; Nakai et al., 2014).

The memory timescale is commonly determined from the autocorrelation function of root-zone soil moisture time series and acts as one measure of the time that it takes for a soil column to forget its initial soil moisture state (Ghannam et al., 2016; Katul et al., 2007; Nakai et al., 2014). Such memory timescale is largely controlled by the loss terms that include evapotranspiration (ET) and drainage below the rooting zone as well as the root-zone depth (Katul et al., 2007). Persistence is the probability that the soil moisture remains in a prescribed state such as wet or dry. The state is selected using root-zone soil moisture or degree of saturation value that marks the crossover between wet and dry phases (s^*) as discussed elsewhere (Ghannam et al., 2016). Dry period persistence is the probability distribution of contiguous durations for which the soil moisture is below some preset threshold (s^*). This definition differs from other widely used definitions such as frequency of daily temperature crossing a given threshold (heat wave persistence) and precipitation anomaly (drought persistence) that have been employed in prior studies (Lorenz, Jaeger, & Seneviratne, 2010; Moon, Gudmundsson, & Seneviratne, 2018). Persistence is inherently stochastic with non-linear dependence on both precipitation (the forcing) and the loss term (evaporation, root-water uptake and drainage) from the root zone (Ghannam et al., 2016), whereas memory depends on the timescale of the losses.

Interconnectedness between rainfall pulses (hours) and rapid fluctuations in the active leaf area of the herbaceous layer (days) makes explorations of memory and persistence in savannas far more challenging than their better studied forested ecosystem counterparts (Ghannam et al., 2016). It is precisely this knowledge gap that motivates the scope of the work here. In a dry savanna ecosystem, root-zone soil moisture is frequently below s^* (i.e. the system is in a persistent dry state). At woodland dominated savannas, soil moisture resides above or close to the water-stress point during the entire wet season (i.e. bistable states in vegetation cover). Grazing pressures add another layer of complexity in explaining what controls memory and persistence in savannas. It is clear that beyond seasonality in leaf area index (LAI) common to many forested ecosystems, rapid land-cover changes due to soil moisture stress and/or grazing are partly driven by rainfall patterns. How such rapid land-cover fluctuations in savannas impact soil moisture memory, persistence and any emerging relation between them is the main question to be addressed here.

Previous work analysed the crossing properties of soil moisture below s^* and derived analytical expressions for the mean annual duration of the dry periods ($\bar{T}_*$) (Porporato, Laio, Ridolfi, & Rodriguez-Iturbe, 2001). The aforementioned analysis shows that the mean dry period is a non-linear function of storm frequency. Motivated by these studies, another aim here is to explore the utility of such findings for longer term modelling of soil moisture variability using measured precipitation. This exercise enlightens possible connection between mean annual duration of soil moisture dry phases and precipitation statistics for multiple water balance models.

To address these overall questions, simplified hydrological models similar to the ones used in previous savanna studies (Miller et al., 2007; Yin et al., 2014) are proposed to interpret measured soil moisture temporal variability at four different savanna land-cover types: grass, grazed, tree and miombo. These sites are chosen owing to the availability of high frequency rainfall and soil moisture time series at high resolution (minimum 2 years at 30-min sampling interval for three sites), eddy-covariance measurements of ET and normalized difference vegetation index (NDVI). All sites report mean rooting depth and soil type thereby constraining estimates of deep drainage losses. The hierarchy of models includes Model 1 with constant maximum daily ET, Model 2 with NDVI adjustment to the ET and Model 3 with NDVI and radiation-based potential ET (PET) adjustment to maximum daily ET. The models proposed accommodate variability in precipitation, ET and NDVI controls on it, as well as radiative components impacting potential ET. By suppressing variability in key land-cover and climatic variables such as NDVI and PET, it is possible to unravel their contribution to soil moisture variability.

2 | METHOD

The hydrological balance approach used to explore variables impacting soil moisture memory and distributions of dry periods (dry period persistence) is first described. Next, the spectral method for time series analysis and the four sites is featured. Details about the method of analysis and its application to soil moisture have been reviewed elsewhere (Ghannam et al., 2016; Nakai et al., 2014), and only salient points are presented here.

2.1 | The soil water balance and definitions

The one-dimensional continuity equation for water in soil including root-water uptake S_R can be expressed as

$$\frac{\partial \theta}{\partial t} = -\frac{\partial q_w}{\partial z} - S_R, \tag{1}$$

where θ is a layer-averaged volumetric soil moisture content (volume of water per unit volume of soil), q_w is the water flux (volume of water per unit ground area per time) assumed to be positive downwards, z is the vertical distance to the soil surface (set at $z = 0$) and t is time. To arrive at a lumped representation of root-zone soil moisture, vertical integration of Equation 1 from $z = 0$ to the root-zone depth $z = Z_r$ is necessary and yields

$$\int_0^{Z_r} \frac{\partial \theta}{\partial t} dz = q_w(0) - q_w(Z_r) - \int_0^{Zr} S_R \, dz, \tag{2}$$

where $q_w(0)$ can be interpreted as either soil evaporation (negative) in the absence of rainfall or throughfall and stemflow lumped together as infiltration (positive) entering the soil surface presumed to be supply controlled and given as $q_w(0) = \gamma P$ for $P > 0$, γ is set to a constant and depends on the interception by the overlying vegetation, P is the precipitation, $q_w(Z_r)$ is the drainage flux from the rooting zone and may be determined from Darcy's law and $\int_0^{Zr} S_R dz$ is the total root-water uptake. For steady-state conditions within the plant system (i.e. no plant capacitance in the root xylem), $\int_0^{Zr} S_R dz$ also determines the transpiration rate. Interchanging the differential and integral operations (Leibniz's rule) on the left-hand side of Equation 2 yields a lumped budget equation for the stored water in the rooting zone given as

$$\frac{d}{dt}\int_0^{Z_r} \theta dz = \frac{dW_s}{dt} = \gamma P - \left(q_w(Z_r) + \int_0^{Zr} S_R \, dz \right), \tag{3}$$

where $W_s = \eta Z_r s(t)$ now defines the stored water within the rooting zone, η is the soil porosity (pore space volume to total volume) and s is the degree of saturation defined by the ratio of the volume of water per total pore (air and water) volume ($s = 1$ implies all pore space is filled with water). When lumping all losses together into a single term $L(t) = q_w(Z_r) + \int_0^{Zr} S_R dz$ and upon assuming that

$$\left| s \frac{d(\eta Z_r)}{dt} \right| \ll \left| (\eta Z_r) \frac{ds}{dt} \right|, \tag{4}$$

the widely used lumped hydrological balance is recovered and is expressed as (Rodríguez-Iturbe & Porporato, 2007)

$$\eta Z_r \frac{ds(t)}{dt} = \gamma P(t) - L(t). \tag{5}$$

This balance links the statistics of $P(t)$ to $s(t)$ provided that a relation between $L(t)$ and $s(t)$ is available or can be obtained from a combination of data and models.

2.2 | Approximations to the soil water balance

The inclusion of land-cover dynamics and meteorological drivers is now discussed by a sequence of approximations to $L(t)$ with the goal of maintaining minimum number of 'tunable' parameters in all of them. These approximations form a hierarchy of models labelled Models 1 to 3. Model 1, the most conventional and widely used in savannas, only considers variability in P holding land-cover type and other climatic drivers constant. Model 2 accommodates NDVI(t) variability on maximum ET only, which then is allowed to impact variability in soil moisture through $L(t)$ and γ. Model 3 assumes that the energy balance and NDVI jointly impact soil moisture so that subdaily timescales as well as seasonality in radiation can introduce additional variability in soil moisture.

In Model 1, $L(t)$ is represented by a piecewise function given as (Laio, Porporato, Ridolfi, & Rodriguez-Iturbe, 2001; Yin et al., 2014)

$$L = ET + D_r = \begin{pmatrix} 0, & s \le s_w, \\ E_{max}\dfrac{s - s_w}{s^* - s_w}, & s_w < s \le s^*, \\ E_{max}, & s^* \le s \le s_{fc}, \\ E_{max} + K_{sat}\left(\dfrac{s - s_{fc}}{1.0 - s_{fc}}\right)^c, & s_{fc} \le s \le 1, \end{pmatrix} \tag{6}$$

where s_w is the wilting point, s_{fc} is the field capacity and the subsurface drainage below the rooting zone is represented by a saturated hydraulic conductivity K_{sat} and an exponent c that varies with soil type (or pore structure) and E_{max} is maximum ET set to a constant assumed to be independent of NDVI or climatic factors. This model remains widely used in semiarid ecosystems (Porporato et al., 2001) for daily timescale analysis and is adopted here as a 'reference' given that its original testing was conducted for African savannas (Laio, Porporato, Fernandez-Illescas, & Rodriguez-Iturbe, 2001). In this model, the drainage flux $q_w(Z_r)$ only varies with the stored water within the rooting zone and not the local soil moisture at $z = Z_r$. This approximation may be an issue that can only be 'bypassed' if the local soil moisture at $z = Z_r$ and the depth-averaged root-zone soil moisture linearly relate to each other as time changes. Also, only gravitational drainage below the rooting zone is considered in the aforementioned $q_w(Z_r)$

(i.e. unit-gradient assumption), which may not be realistic at all times (Katul, Wendroth, Parlange, Puente, & Nielsen, 1993). The maximum ET ($E_{max,EC}$) and s^* can be independently determined using eddy-covariance measurements of water vapour flux. When forming bins of measured ensemble-averaged soil moisture along with their ensemble-averaged ET in increasing order, the rightmost bin of the linear increase in daily ET as a function of bin average daily mean soil moisture defines the plant water-stress threshold (s^*), and the corresponding ET value is the $E_{max,EC}$. The s_w is also set to the lowest observed value of s in each year, and the s is constrained to this value (i.e. all losses go to zero) to avoid unrealistic soil moisture levels for the models. For model comparison, the percentage of drainage, ET loss under water stress (ET_s) and nonstressed ET (ET_{ns}) were calculated. The ET_s is the ET loss when soil moisture is below s^* (water limitations impact transpiration), and ET_{ns} is the ET loss when soil moisture is above s^* (no water limitations).

Model 2 expands Model 1 by allowing maximum daily ET to vary with NDVI as (Yin et al., 2014)

$$E_{max} = a_2[1-\exp(-bNDVI)], \tag{7}$$

where a_2 is a fitting parameter and the b parameter is an extinction coefficient for global radiation set to 0.4 for Models 2 and 3 (Al-Kaisi, Brun, & Enz, 1989; Teuling, 2005).

Model 3 further expands on Model 2 by allowing a radiation-based PET (=*PET*) and NDVI to jointly impact maximum ET rate at subhourly timescale so that

$$E_{max} = a_3[1-\exp(-bNDVI)]PET, \tag{8}$$

where a_3 is another fitting parameter and PET is determined (at subhourly timescales) using the Priestley–Taylor formulation (Priestley & Taylor, 1972)

$$PET = \alpha_{PT}\frac{\Delta}{\Delta+\gamma_p}(Rn-G), \tag{9}$$

where α_{PT} = 1.26 is the Priestley–Taylor coefficient, Δ is the slope of the Clausius–Clapeyron equation with respect to temperature evaluated at the measured air temperature and γ_p is the psychrometric constant. In Models 2 and 3, variability in NDVI also impacts interception (discussed later). Model 3 allows both seasonal and diurnal variation in radiation to impact soil moisture variability.

The model parameters were fitted following a sequence of steps. The K_{sat} values were chosen based on published soil type for the site. The s_{fc} was set to $s^*/0.75$. The relation between the s_{fc} and the drainage parameter c may be different at the sites, and thus, the parameter c was fitted for each site by minimizing the root-mean-square error (RMSE) of measured, and Model 1 based soil moisture during drainage periods only. These drainage parameters were also used for Models 2 and 3 for consistency. The a_2 and a_3 parameters were fitted by minimizing the RMSE of measured and modelled soil moisture.

2.3 | Interception

Part of the rainfall does not enter the soil but is intercepted by the vegetation and re-evaporated rapidly (ponding and overland flow are ignored in this analysis). For semiarid areas, this loss can be substantial owing to the high evaporative demand by the atmosphere. Hence, the constant γ was determined based on the amount of measured soil moisture increases during measured precipitation events. The numerical value of γ was computed by regressing the cumulative measured increases in soil moisture during precipitation events against measured cumulative precipitation. The rainfall and soil moisture time series used in the calculation of γ were determined by taking the soil moisture increases from the start of an isolated rainfall event until 24 h after the termination of the event. Naturally, γ lumps multiple sources of errors, including the representativeness of the rainfall measurements at the gauge of the rainfall experienced by the soil moisture probes, the precise placement of the soil moisture sensors and any near-surface evaporation. Its numerical value cannot be strictly viewed as 'hydrological' and must be interpreted within the context of such spatial scale-mismatch between measured precipitation and root-zone soil moisture at two separate locations. Nonetheless, because measured point precipitation is used as the main driver in the three hydrological balance models, it is necessary for parameter γ to absorb these space scale-mismatch issues.

2.4 | Memory, persistence and spectra

The term $ds(t)/dt$ in Equation 5 is linked to the storage of water in soil pores, thereby introducing memory (Delworth & Manabe, 1988; Ghannam et al., 2016; Katul et al., 2007; Parlange et al., 1992). Memory (or integral timescale) of a stochastic variable can be determined from the area under the autocorrelation function of a time series given as

$$\tau = \int_0^{+\infty} \rho_s(\alpha)\mathrm{d}\alpha, \tag{10}$$

where α is the time lag and $\rho_s(\alpha)$ is the autocorrelation function of time series $s(t)$ when stationarity is assumed (Priestley, 1981).

The wet and dry states can be defined from soil moisture time series by setting an indicator function to unity when soil moisture is deemed as wet and zero otherwise. Such binary time series of the indicator function are referred to as the telegraphic approximation (TA) of the full soil moisture time series. The plant water-stress (s^*) is used to delineate the threshold between wet (TA = 1) and dry (TA = 0) states.

The normalized spectra of soil moisture ($E_{ns}(f)$) and precipitation ($E_{np}(f)$) are the Fourier transforms of their corresponding autocorrelation functions. These spectra were estimated using the Welch averaged modified periodogram method (Welch, 1967). The window length for the spectral estimation varied from 130 to

268 days for the different measurement sites depending on the record duration. An analytical relation also exists between precipitation and soil moisture spectral exponents for a linear $L(s)$. When a constant (or white-noise) spectrum ($(E_{np}(f)$ = constant) for rainfall is assumed, the soil moisture spectrum decays as a red-noise spectrum (i.e. f^{-2}) at high frequencies (Katul et al., 2007; Nakai et al., 2014) and becomes flat at very low frequencies (i.e. f^0). The measured precipitation spectrum, which exhibits spectral decay from $f^{-0.5}$ to f^{-1} at high frequencies (daily to subdaily), adds to the decay rate of soil moisture spectrum, making it resemble 'black' instead of 'red' noise (Ghannam et al., 2016; Katul et al., 2007; Nakai et al., 2014). When the spectra of soil moisture and its *TA* time series exhibit power laws of the form $E_{ns}(f) \sim f^{-n}$ and $E_{TA}(f) \sim f^{-m}$, there exists an empirical relation between the spectral exponents given by

$$m = \frac{n+1}{2}, \tag{11}$$

where n is the spectral exponent of soil moisture and m is the spectral exponent of the *TA* of soil moisture (Cava & Katul, 2009; Cava, Katul, Molini, & Elefante, 2012; Molini, Katul, & Porporato, 2009; Sreenivasan & Bershadskii, 2006). This measure identifies to what extent the soil moisture memory is related to the switching between wet and dry or dry and wet (i.e. binary state) instead of temporal variations within the wet state.

Persistence is defined as the distribution of time periods when the soil moisture TA series does not change sign. Specifically, the dry persistence is the probability density function (PDF) of periods when the value of soil moisture is below the s^* threshold. These periods are forced by the interaction between precipitation distribution and the total loss term in the water balance equation. To compare dry persistence between the various measurement sites, the distribution of dry periods is normalized by the memory timescale, and a stretched exponential function (Laherrère & Sornette, 1998) is fitted to the data. This function is given as

$$\mathrm{PDF}(x) = A_x x^{\beta-1} \exp\left(-x^{\beta}\right), \tag{12}$$

where $x = (I_{dry}/\tau)$ are the dry periods normalized by the memory timescale, $A_x = \beta \exp\left(x_{min}^{\beta}\right)$ is a normalizing constant needed to ensure that $\int_0^{\infty} PDF(x)\,dx = 1$ and x_{min} is the shortest dry period. The fitting parameter β is assumed to be less than unity. Lower values of β indicate that long water-stress periods decay closer to a power law, whereas higher β indicates exponential decay at long times. In stochastic analysis of the water balance, the mean annual duration of the dry periods ($\bar{T}_*$) represents the long-term average annual dry period (Porporato et al., 2001). Here, $\bar{T}_*$ was estimated for the modelled soil moisture series covering only full hydrological years by first taking the mean of dry periods of each hydrological year and then calculating the mean and standard deviation of the annual T_* values.

2.5 | Rainfall characteristics

For across site comparison purposes, daily mean precipitation depth (P_α mm/event) and daily mean storm frequency (P_λ events/day) are used to describe the mean storm characteristics (Rodriguez-Iturbe, Porporato, Ridolfi, Isham, & Coxi, 1999). The mean precipitation depth was calculated only for rainy days. The mean storm frequency was calculated from inverse of the mean time between rainy days. The reported precipitation statistics here may not represent long-term mean precipitation statistics given that the records span only few years.

2.6 | Sensitivity analysis

Sensitivity of Model 3, which is considered as a reference model capturing soil moisture variance, was tested by running the model with ±20% different s^* values at 10% increments at all sites. The s_{fc} was also set accordingly to $s^*/0.75$. This s^* percentage range is the same as the difference between the s^*values of the different grass species at Nylsvley savanna in South Africa (Laio, Porporato, Fernandez-Illescas, & Rodriguez-Iturbe, 2001). In addition, each model run was conducted with ±20% different precipitation by increasing or decreasing measured precipitation. For each value of s^*, the standard deviation of modelled memory timescale was estimated from the simulations with different precipitation. The sensitivity of dry persistence parameter β to the total precipitation amount was also estimated from the simulations with different precipitation amounts.

To quantify the sensitivity of soil moisture memory on rainfall statistics, stochastic rainfall was generated from a Poisson process at each site. This sensitivity test was conducted using Model 2 because the tree savanna net radiation measurement had missing periods during the 5-year simulation period. The stochastic simulations from Models 2 and 3 were compared at the grazed savanna and showed that the mean Model 3 memory timescale differed from Model 2 mean memory timescale by less than one standard deviation. The synthetic precipitation series were constructed with precipitation intensity similar to the measured intensity from long-term records. Random daily rainfall series were generated assuming that times between rainfall events are exponentially distributed with mean $1/P_\lambda$, and the depth of daily rainfall is exponentially distributed with mean depth P_α (Laio, Porporato, Ridolfi, & Rodriguez-Iturbe, 2001). The random rainfall series were generated at a daily scale for 5-year period; then constant period of zero rainfall was set to each year corresponding to typical dry season length. The dry season length was 180, 120, 110 and 180 days for grass, grazed, tree and miombo savannas, respectively. From these rainfall series, only the ones with precipitation intensity near the observed one (±0.1) were used in the simulations. Model 2 was run with 50 different random rainfall series to generate memory estimates, and the mean and standard deviation of all memory estimates were calculated. The same model parameters were used as described above, but the model was stepped in daily timestep with the exception that on days when s + infiltration was higher than s_{fc},

the soil moisture was reduced owing to drainage in hourly timesteps (Pumo, Viola, & Noto, 2008). The site NDVI time series from September 2010 to August 2015 were used at each site.

2.7 | Measurement sites

The measured root-zone soil moisture time series were collected at four African savanna sites with grass, grazed, tree and miombo savanna vegetation cover (Figure 1). Eddy-covariance measurements of *ET* were used to determine plant water-stress levels at all sites on the basis of a relation between daily averaged relative soil moisture and measured ET. The site characteristics and model parameters used for each site are summarized in Table 1.

The grass savanna site in Kenya is located close to a maize farm and presents a site with no influence of tree roots. The soil moisture profile measurements were conducted inside a fenced meteorological station. During the long rainy season, grasses grow inside the fenced area and impact soil moisture.

The Welgegund grazed savanna site has perennial grasses growing around the soil moisture measurement location, and the area is used for grazing livestock (Jaars et al., 2014, 2016, 2018; Räsänen et al., 2017). The eddy-covariance footprint has some 15% tree cover, and some tree roots were identified at 40-cm depth nearby the soil moisture measurements.

The tree savanna measurement site is located near Skukuza within Kruger National Park. This site is grazed and browsed by ungulates (Scholes et al., 2001). The soil moisture measurements were taken from the *Combretum apiculatum*-dominated savanna. The grasses and trees access soil water throughout the soil profile, but grasses use shallow soil water more efficiently than trees. Trees can shift the water uptake from shallower depths to deeper depths (Archibald et al., 2009; Kulmatiski & Beard, 2013). The tree canopy cover around the area is about 30% (Archibald et al., 2009).

The miombo savanna site is located within the Kataba Forest Reserve in Zambia (Kutsch et al., 2011). It is a woodland savanna characterized by a canopy cover of nearly 70%. The soil moisture profile was located at an open canopy. Because of missing precipitation during the second year, the analysis is restricted to the first year only, which is a major drawback for the inclusion of this site. Hence, the analysis from this site must be viewed with the usual cautionary notes associated with short-measurement records and convergence of statistics.

At each site, precipitation pulses and soil moisture increases had similar timing. For this reason, precipitation time series at the Skukuza measurement site was gapfilled based on observed relative soil moisture (SI1). The grass savanna net radiation was estimated from measured incoming radiation and soil heat flux using empirical functions from an ET from relative humidity in equilibrium (ETRHEQ) model (Rigden & Salvucci, 2017). The relative soil moisture was determined from volumetric soil moisture measurements up to depths of 30, 40, 29 and 50 cm for the grass, grazed, tree and miombo savannas, respectively. The longest gaps in relative soil moisture time series ranged from 3 h at the grass savanna to 25 days at the miombo

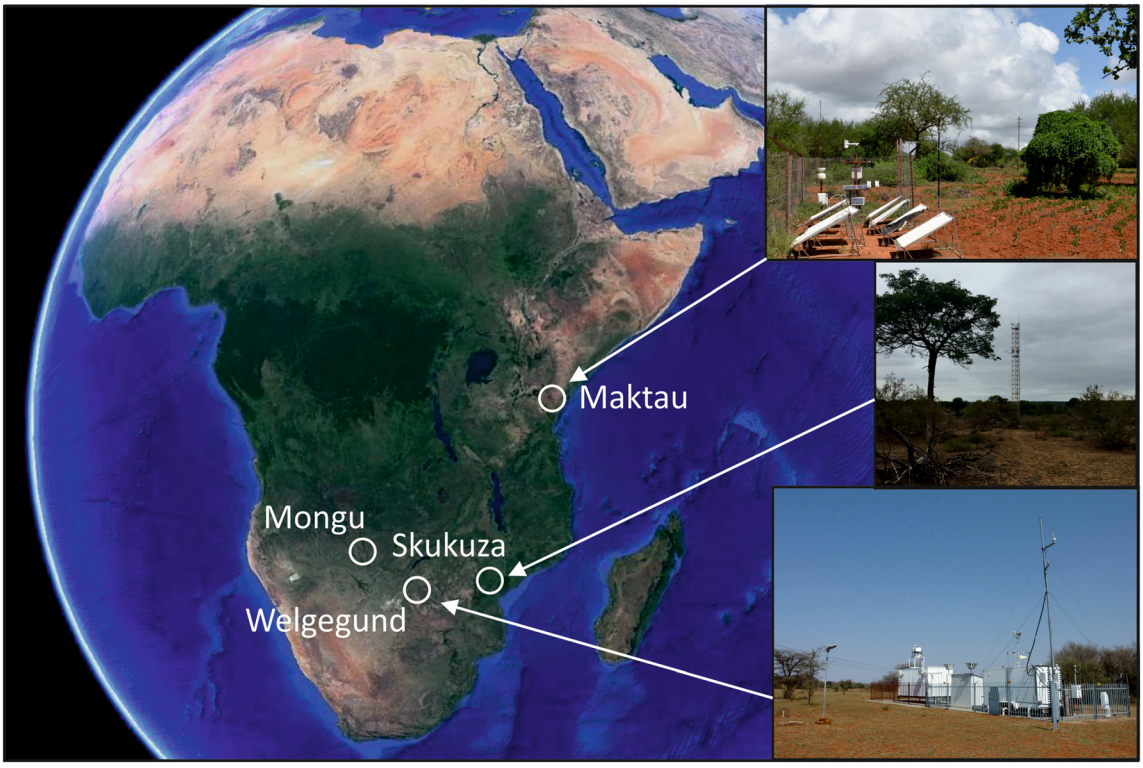

FIGURE 1 Location of the study areas: a grass savanna (Maktau, Kenya), a grazed savanna (Welgegund, South Africa), a tree savanna (Skukuza, South Africa) and a miombo savanna (Mongu, Zambia). Figure design by P. Pellikka

TABLE 1 Site description

Land use	Grass savanna	Grazed savanna	Tree savanna	Miombo	Source
Country	Kenya	South Africa	South Africa	Zambia	
Site	Maktau	Welgegund	Skukuza	Mongu	
Coordinates	3°25′32″S, 38°08′21″E	26°34′10″S, 26°56′21″E	25°01′10″S, 31°29′49″E	15°26′15′S, 23°15′09″E	
Long-term mean annual precipitation (mm)	433	572	550[a]	948	
Soil texture	Sandy clay loam	Loamy sand	Sandy loam	Kalahari sand	
Soil porosity (η)	0.43	0.42	0.43	0.44	
Soil moisture measurement depths (cm)[b]	**10**, **30**, 50	**10**, **20**, **30**, **40**, 60, 100	**6**, 13, **29**, 48	**5**, **30**, **50**, 100	
Mean root-zone depth (Z_r) (mm)[c]	300	400	290	500	
Ratio of precipitation entering the soil (γ)	0.48	0.6	0.73	0.6	Calibration (Figure 3)
Water-stress point (s^*)	0.33	0.35	0.25	0.11	Eddy covariance
Max ET ($E_{max,EC}$) (mm/day)	1.5	3.3	3.4	2.8	Eddy covariance
Field capacity (s_{fc})	0.44	0.46	0.33	0.15	$s_{fc} = s^*/0.75$ (Ghannam et al., 2016)
Mean wilting point (s_w±SD)	0.1 ± 0.009	0.18 ± 0.023	0.12 ± 0.002	0.01	Measured s
Saturated hydraulic conductivity (K_{sat}) (cm/day)	80	100	80	1,272	(Laio, Porporato, Fernandez-Illescas, & Rodriguez-Iturbe, 2001; Wang, D'Odorico, Ringrose, Coetzee, & Macko, 2007)
Drainage parameter (c)	1.3	2.6	2.2	2.5	Fit by minimizing RMSE during drainage
Extinction b	0.4	0.4	0.4	0.4	Teuling (2005)
Model 2 parameter a_2	0.6	0.7	0.5	0.3	Fit by minimizing RMSE
Model 3 parameter a_3	2.6	4.0	3.1	1.1	Fit by minimizing RMSE
NDVI (mean/min/max)	0.40/0.25/0.61	0.36/0.23/0.64	0.36/0.20/0.72	0.60/0.41/0.69	
$\overline{PET}_{max}\left(\frac{mm}{day}\right)$	7.9	5.9	8.4	6.7	
Mean precipitation depth (P_α) (mm/event)	4.6	6.4	7.0	8.4	
Mean storm frequency (P_λ) (events/day)	0.24	0.22	0.13	0.19	
Mean precipitation intensity ($P_\alpha \cdot P_\lambda$) (mm/day)	1.1	1.4	0.9	1.6	
The longest gap in relative soil moisture	3 h	11 d	2 d	25 d	
Measurement period	Oct 2013–April 2019	Apr 2012–Jan 2018	Feb 2015–Dec 2017	Sep 2007–Sep 2008	
References	Not previously published	Jaars et al. (2016; Räsänen et al., 2017)	Scholes et al. (2001); Archibald et al., 2009)	Kutsch et al. (2011)	

[a]280 mm during the measurement period.
[b]Bolded depths were used for calculating relative soil moisture. Soil moisture sensors were Campbell CS650 (Maktau), Delta-T PR2 (Welgegund), Campbell CS615 (Skukuza) and Delta-T ThetaProbe (Mongu).
[c]Estimated from field sampling. At Skukuza and Mongu site, this is limited by the availability of soil moisture data.

savanna (Table 1). The longest gaps in precipitation coincided with gaps in soil moisture except for the tree savanna site. During these periods, precipitation was set to zero. To construct a longer precipitation series for estimating mean annual dry period, the tree savanna precipitation was used from 2011 to 2016. This period had gaps in soil moisture and one additional 25-day gap in November 2013 during which the precipitation was set to zero.

Each site had an eddy-covariance system measuring ET using a triaxial sonic anemometer and an infrared gas analyser (Table 2). An open-path analyser was used at the tree savanna, whereas other sites had a closed-path sensor. The latent heat flux was calculated using standard eddy-covariance procedures at each site (Archibald et al., 2009; Kutsch et al., 2011; Räsänen et al., 2017). The time series of latent heat fluxes were gapfilled using an artificial neural network using soil temperature, incoming global radiation, soil moisture and NDVI (Isaac et al., 2017). The latest FLUXNET2015 (http://fluxnet.fluxdata.org) eddy-covariance data were used at the tree and miombo savanna sites (Pastorello et al., 2017). At these sites, the flux gapfilling algorithm used was based on the marginal distribution sampling procedure (Reichstein et al., 2005). Only days when there were at least 4 h of daytime measured fluxes were used for the determination of the plant water-stress level. The eddy-covariance data during the soil moisture measurements were used for all sites except the tree savanna site where the year 2009–2010 data were used instead.

The NDVI time series were generated at each site on the basis of MODIS collection 6 NDVI 250 m product (MOD13Q1) as discussed elsewhere (Didan, 2015). The original 16-day interval time series were smoothed using Savitzky–Golay filter and linearly interpolated to 1-h timestep for Models 2 and 3 (Isaac et al., 2017).

3 | RESULTS

3.1 | Data and model results

3.1.1 | Precipitation

The annual precipitation at the tree savanna site was about 50% less than at the grazed savanna site during the two growing seasons covering the tree savanna site measurements (Table 1). During these years from 2015 to 2017, South Africa experienced a drought, and the precipitation was exceptionally low at the tree savanna site. The long-term annual precipitation of the tree savanna site is 550± 160 mm (Archibald et al., 2009), whereas during the measured period, mean annual precipitation (MAP) was only 280 mm.

3.1.2 | Normalized difference vegetation index

The short (Nov–Jan) and long (Feb–May) rainy seasons are present as peaks in the NDVI time series at the grass savanna (Figure 2). The years 2017–2018 also have the lowest peak NDVI value at this site. The grazed and tree savanna sites have similar bimodal trends in NDVI during the drought years 2016–2017. These drought year peak NDVI values are among the lowest annual peak values of the entire time series starting from the year 2000 for the grazed and tree savannas. The grazed site is dominated by the perennial grass that experiences dieback and regrowth during this drought year.

3.1.3 | Evapotranspiration

The daily PET has a stronger seasonal cycle at the South African sites than at the miombo and grass savannas (Figure 2).

For the grazed, tree and miombo savanna sites, the bin averaged relation between mean daily soil moisture and eddy covariance-based ET shows clear saturation. For the grass savanna, this saturation pattern is not evident. The grass savanna had the lowest E_{max} (1.5 mm/day) value of all the sites considered here. The grazed and tree savannas had similar $E_{max,EC}$ (3.3 and 3.4 Mm/Day) but different s^* values (0.35 and 0.25).

3.1.4 | Interception/re-evaporation losses

To match the measured soil moisture increases with measured precipitation input, the loss term γ was determined from the relation

TABLE 2 Eddy-covariance set-up and gapfilling algorithms used for micrometeorological measurements.

Site	Height (m)	Sonic anemometer	Gas analyser	Data period	Missing data (%)	Gapfilling algorithm
Grass	6	USA-1 (METEK)	Closed path LI-7200 (LI-COR)	2016	52	Neural network
Grazed	9	USA-1 (METEK)	Closed path LI-7000 (LI-COR)	2012–2016	41	Neural network
Tree	16	CSAT-3 (Campbell Scientific)	Open path LI-7500 (LI-COR)	2009–2010	34	Marginal distribution sampling
Miombo	19	R3 (GILL Instruments Ltd.)	Closed path LI-7000 (LI-COR)	2007–2009	54	Marginal distribution sampling

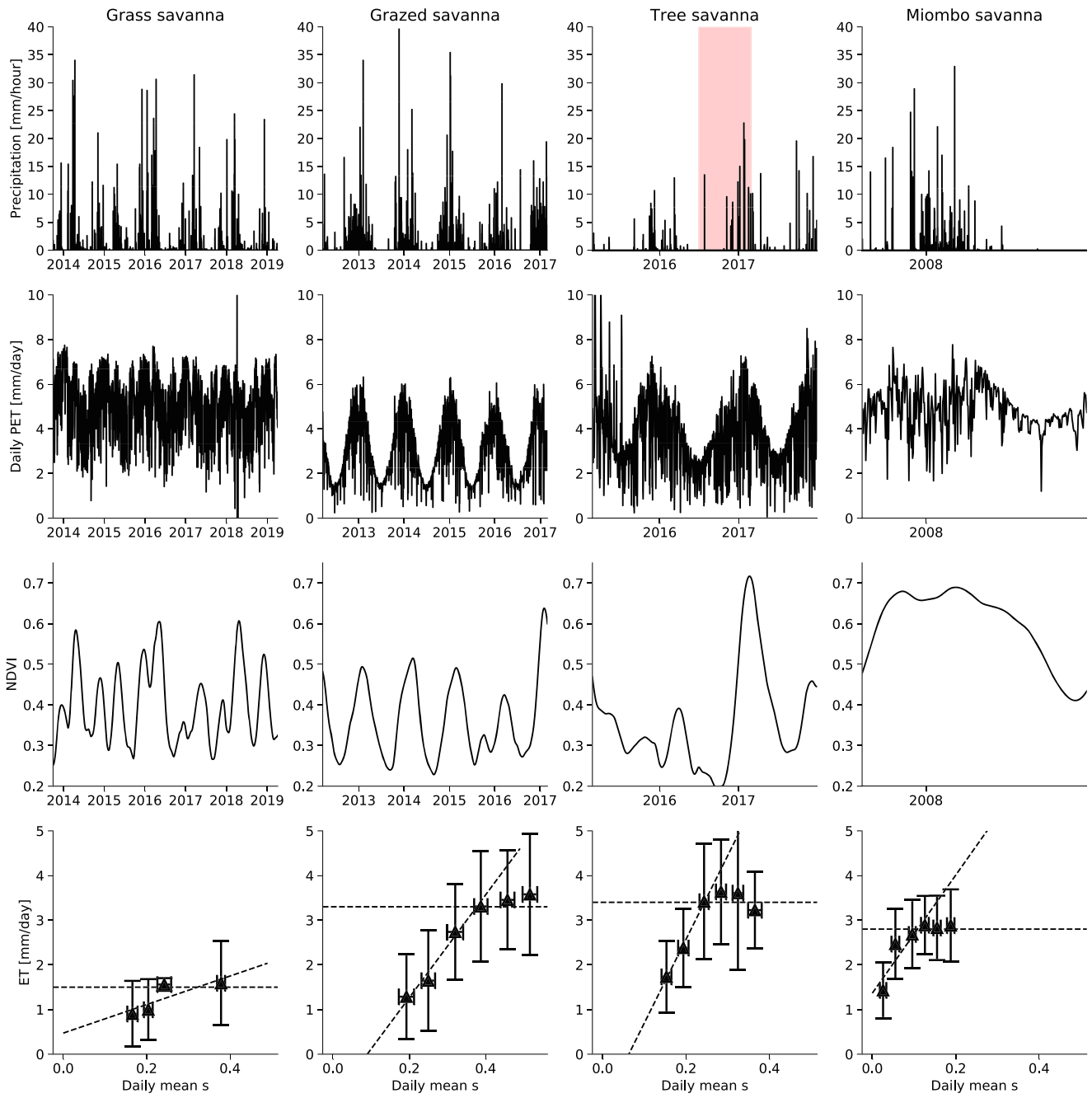

FIGURE 2 Time series of measured precipitation, potential evapotranspiration (PET) and normalized difference vegetation index (NDVI) at the grass, grazed, tree and miombo savannas. The red background indicates period of gapfilled precipitation at the tree savanna site. The last row shows the relation between measured daily mean soil moisture and eddy covariance-measured evapotranspiration. The rightmost bin of the linear increase in ET defines the plant water-stress threshold (s^*) and $E_{max,EC}$

between cumulative rainfall and rain-related soil moisture increases at all sites (Figure 3). As noted earlier, this term represents interception loss and re-evaporation from soil surface but also all the spatial variability linking rainfall and local soil moisture changes at differing points in space. Its numerical value was the lowest at the grass savanna site. At the grazed savanna site, there was a deviation from the assumed linear relation when cumulative rainfall was around 1,000 and after 2,400 mm. At the tree and miombo savannas, the relation was non-linear at the beginning of the wet season but maintained linearity thereafter. A non-linear relation here is suggestive that γ may not be constant and can depend on rainfall amounts. However, given uncertainties in measured rainfall and the concomitant rapid increases in soil measurements, a constant value of γ was selected for maintaining maximum model simplicity (in all three models).

Jumps in measured soil moisture largely match in timing jumps in modelled soil moisture at all sites (Figure 4). Furthermore, for

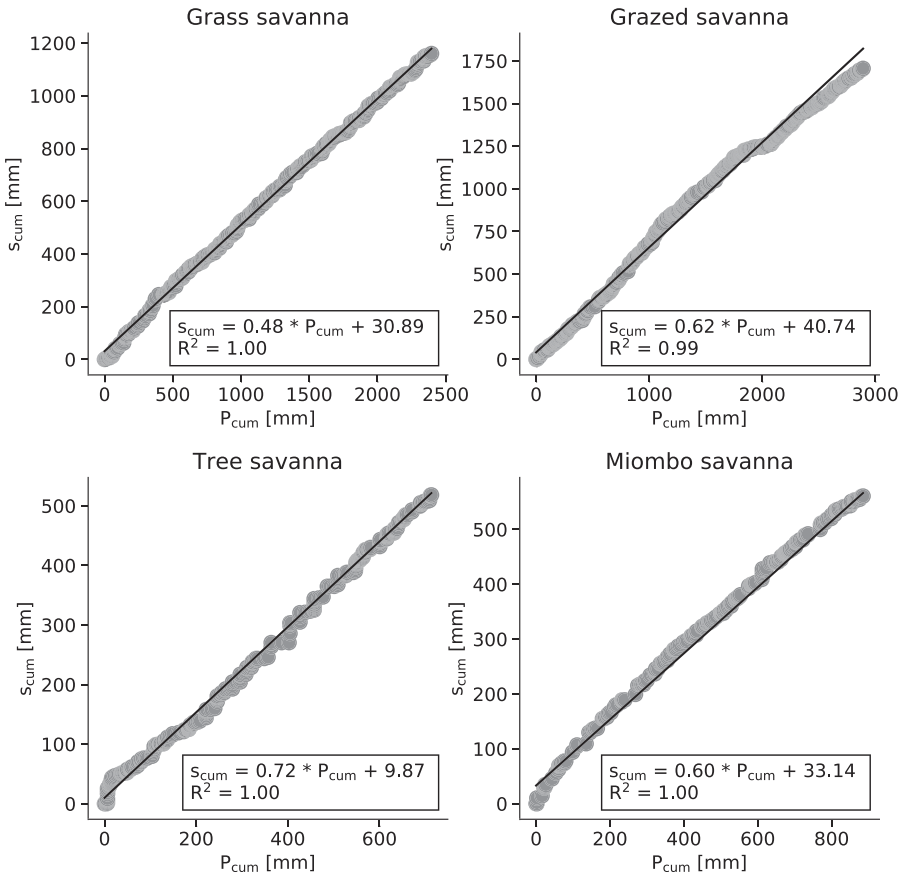

FIGURE 3 Relation between cumulative precipitation and cumulative positive increments in soil moisture for each site. The regression slope determined γ at 48%, 62%, 72% and 60% of the precipitation for the grass, grazed, tree and miombo savannas, respectively

Models 2 and 3, the soil moisture decay rates are comparable with the measured ones. The models deviated from measurements owing to difference either in magnitude of the soil moisture jump or in the low dry season values. The water input was underestimated at the grazed savanna in years 2013–2014 and at the beginning of tree and miombo savanna time series because the interception loss during these times is different from the one estimated by a constant γ (as expected). Also, change in precipitation uncertainty between years could affect the model water input.

3.1.5 | Model results

Model 1, which uses the EC estimated constant E_{max} values, only overestimates ET loss rate resulting in underestimation of soil moisture (as expected). Models 2 and 3 fit the measured soil moisture better at the tree savanna than does Model 1. The changes in interception loss and differences in dry season minimum soil moisture values at the grazed savanna resulted in larger absolute differences between modelled and measured soil moisture values. The aforementioned changes in dry season minimum soil moisture are likely the result of one sensor drift. The soil moisture sensor (Delta-T PR2) at this site is an integrated profile measurement, and the drift is largely due to the 10-cm record. The models underestimate the variability in drainage rate at the miombo savanna and thus overestimate the soil moisture values during the mid-wet season. Visual inspection of the measured soil moisture series at miombo savanna reveals that the shape of the soil moisture decay around the drainage events can vary between subsequent events for similar antecedent soil moisture values.

The models fit the measured soil moisture nearby s^* crossings better at the grass and tree savannas, which have more isolated precipitation events (Table 1 lower $P_\alpha \cdot P_\lambda$) than at the other sites. Model 1 overestimates soil moisture values near the s^* at the grass savanna and underestimates at the tree savanna. At the grazed savanna, all models underestimate soil moisture values near the s^* during the wet years and overestimate during the drought years. At miombo savanna, Model 1 captures better the s^* crossings but overestimates the early wet season ET loss rate. The soil moisture is below the plant water-stress threshold during years 2015 and 2017 wet seasons at the grass savanna, whereas it crosses the s^* even during the drought years at the grazed and tree savannas. However, the in-season dry period in 2015 at the grazed savanna is similar in length to a typical dry season length. At the miombo savanna, the soil moisture is above the threshold during the mid-wet season.

The partitioning of the water loss components shows that Model 1 has a larger percentage of ET under water stress and a lower percentage of drainage at the grazed, tree and miombo savannas (Figure 5). Despite the lower s^* at the tree savanna compared with the grazed savanna, the partitioning of water loss at

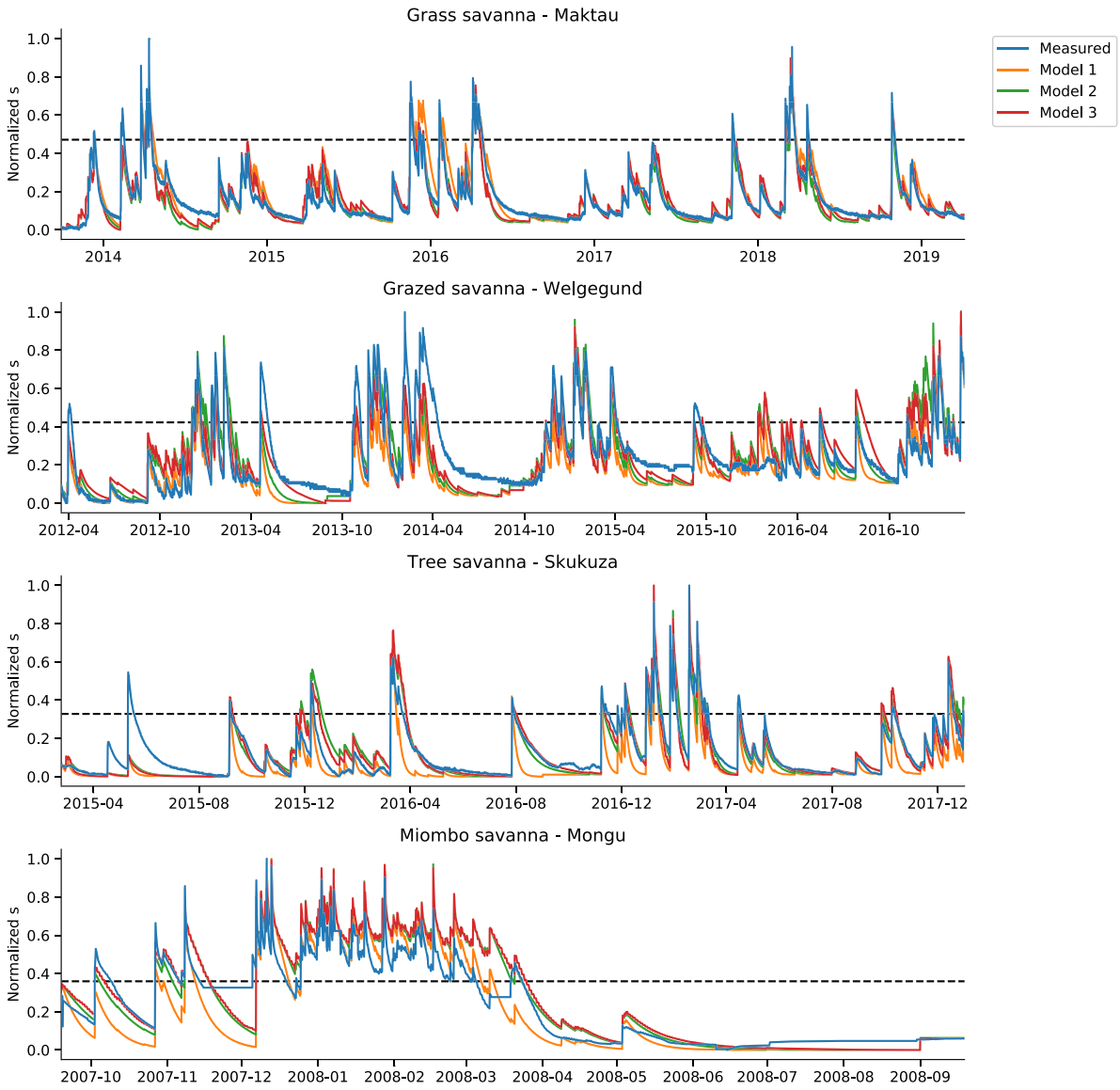

FIGURE 4 Time series of normalized soil moisture. The soil moisture values were rescaled to 0–1 range. The dashed line indicates the normalized value of the water-stress point (s^*)

these sites is similar. At the miombo savanna, the amount of drainage and nonstressed ET loss is higher than the amount of stressed ET loss. Model 3 RMSE was the smallest at all sites (Figure 5) when compared with the other two models. The difference in RMSE between Models 2 and 3 was small also at all sites except the grazed savanna.

The comparison between model and measured soil moisture histograms reveals that the modelled frequency of lower soil moisture bin is higher than measured results at the grass, grazed and tree savannas (Figure 6). This is due to the model underestimation of the dry season soil moisture values. At the grass and tree savannas, the tail of measured and Model 3 histograms are similar. The miombo and, to a lesser extent, the grazed savanna histograms are bimodal. The wet peak is not captured by the models at the grazed savanna, whereas the modelled miombo histograms have a wet peak at higher values than the observed soil moisture series. Models 2 and 3 histograms are similar at the grass, tree and miombo savannas.

3.2 | Precipitation, soil moisture spectra and memory

The measured soil moisture memory timescales were determined to be 21, 31, 17, and 50 days for the grass, grazed, tree and miombo savannas, respectively (Figure 7). The estimated memory for Model 3 soil moisture series is the most consistent with data—with maximum difference between measured and modelled not exceeding 3 days.

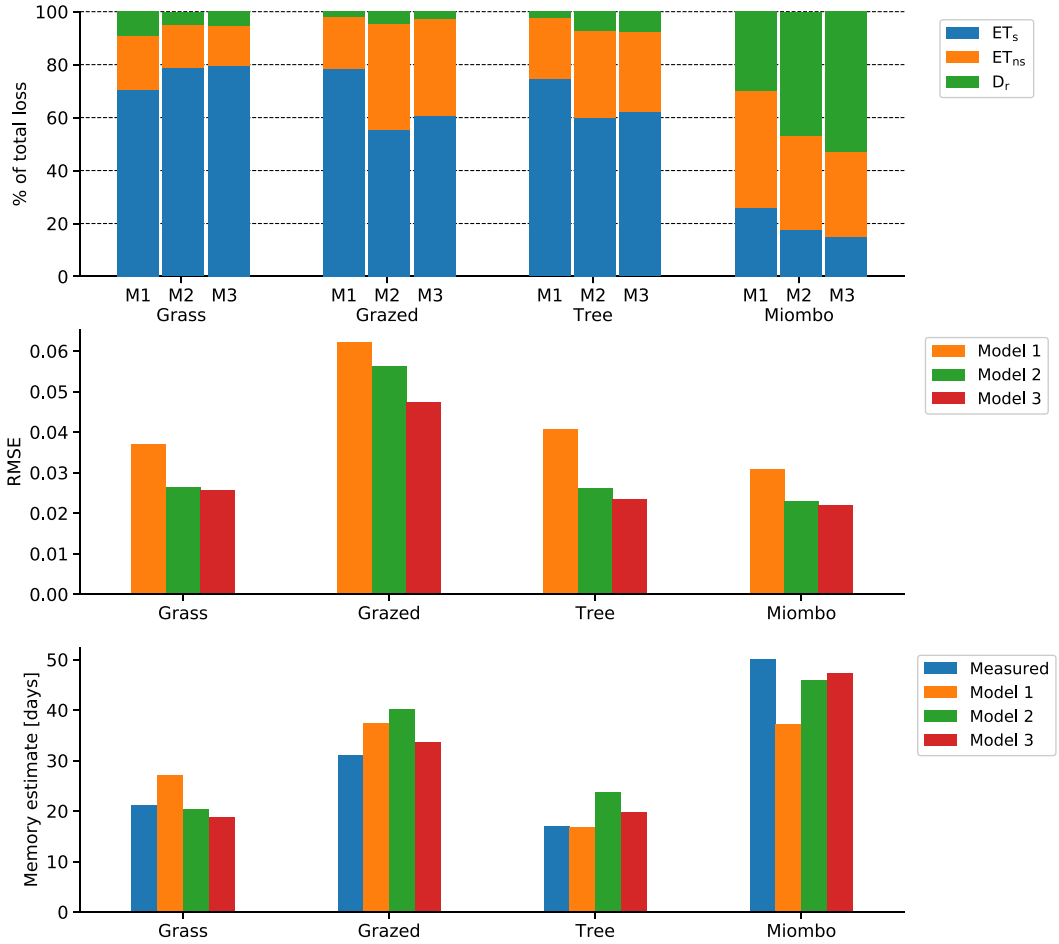

FIGURE 5 Comparison of water loss components, root-mean-square error (RMSE) and memory estimates. The total loss is partitioned to drainage (D_r), unstressed ET (ET_{ns}) and water stress ET (ET_s)

Model 1 has a constant maximum ET that does not change during early or late wet season, and thus, Model 1 overestimates the memory timescale at the grass and grazed savannas. At the tree savanna, Model 1 agrees with measured soil moisture memory despite consistently higher ET loss rates. At this site, storm frequency is low, and Model 1 largely underestimates the wet periods and overestimates periods of low soil moisture. These low periods increase the soil moisture memory, and thus, Model 1 memory is close to the observed memory. Model 3 memory is 2 days higher at this site, and this difference is related to soil moisture differences during the drainage events that were fitted using Model 1. The comparison of two different soil moisture profiles at the grass sites shows that absolute differences in soil moisture profiles do not lead to a difference in soil moisture memory, but at the miombo savanna, the canopy soil moisture profile has 6 days lower memory timescale (Figure S1). It seems that the major difference between miombo open- and closed-canopy soil moisture memory is due to the difference in infiltration and drainage peaks as opposed to ET losses.

At diurnal to daily timescales, the measured precipitation spectrum deviates from white noise and exhibit approximate power-law scaling commensurate with commonly reported values (i.e. exponents varying between $f^{-0.5}$ and f^{-1}). These exponents in the precipitation spectra result in soil moisture spectral exponents that are less than −2 for increased f. The difference between the measured precipitation spectral exponents and measured soil moisture spectral exponent decimals was 0.06, 0.25, 0.38 and 0.39 for the grass, grazed, tree and miombo savannas, respectively (Figure 7). The measured precipitation spectra are 'noisy' at those fine scales, and care must be exercised in overinterpreting the exponents as a signature of precipitation formation (convective closer to $f^{-0.5}$ and frontal closer to f^{-1}).

At every site except miombo savanna, Model 3 soil moisture spectral exponent was higher and closer to the observed, suggesting that spectral exponents describing higher frequencies are driven by additional processes beyond pulsed rainfall. For grass and grazed savannas, the soil moisture spectrum has diurnal peaks that are evident in Model 3 spectra, whereas at the tree savanna, the spectrum does not display peaks. At the grass and grazed sites, the time series were longer (>4 years). This longer record duration makes the soil moisture spectral estimate more robust at seasonal timescales. There is no regime shift in the measured soil moisture spectrum at the seasonal scale across these sites. The scaling laws for soil moisture and

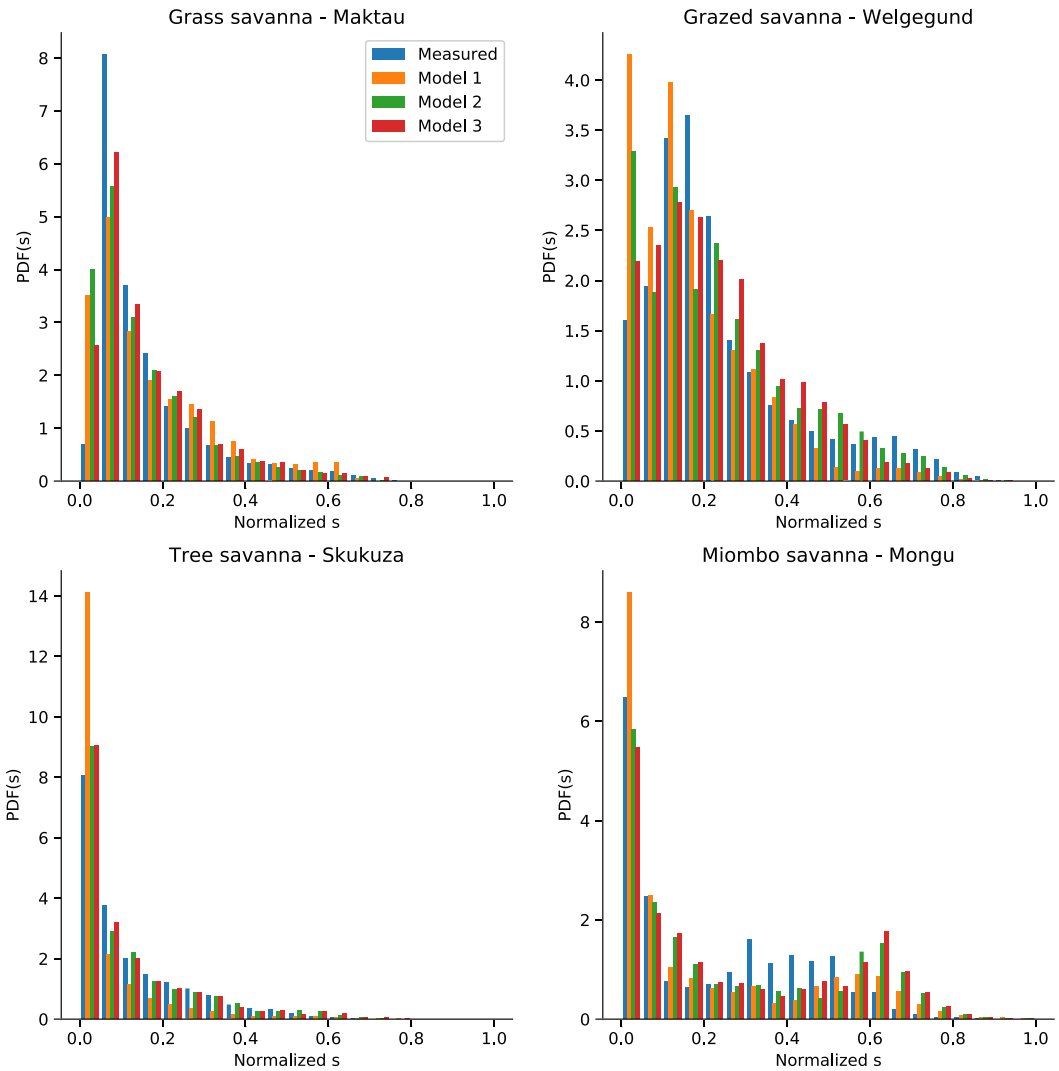

FIGURE 6 Histogram of normalized soil moisture for each savanna. The soil moisture values were rescaled to 0–1 range

its TA series extended from hourly up to soil moisture memory timescale. The largest difference between the TA exponent of soil moisture and the predicted exponent from Equation 11 was 0.08 at the miombo savanna. All models captured soil moisture spectral exponents reasonably. However, Model 3 only overestimated the measured TA exponent by a maximum of 0.04 at the grass, grazed and tree savannas. Given the model simplicity and assumptions, this agreement is encouraging, thereby allowing Model 3 to be used as a 'reference' explaining the main drivers of measured soil moisture variability.

An unforeseen outcome is that the daily mean rainfall intensity and measured memory timescale are linearly related across the three savannas where ET/infiltration $\sim$ 1.0 (Figure 8). This relation would be even more linear if the grazed savanna root-zone depth is the same as at the other sites because lower root-zone depth results to lower memory. The stochastic rainfall simulation of Model 2 has a similar relation, and it shows that the standard deviation of memory at each site is less than memory differences between the sites. The large drainage at miombo savanna leads to a large difference between stochastic Model 2 memory and observed memory because the model cannot recover the drainage peaks at this site.

In summary, Model 1, which accounts for precipitation variability, captures the soil moisture spectral decay at large f. Model 3 with PET adjustments marginally improves the prediction of spectral exponents at high f. However, the memory timescale estimates from Model 3 closely match the measurements. Similar to the RMSE, the differences between Models 3 and 2 memory timescales are the largest at the grazed savanna site.

3.3 | Distribution of dry persistence periods

Figure 9 shows the distribution of times when soil moisture was below the plant water-stress threshold (s^*) normalized by the site-specific memory timescale. The memory timescales and the dry

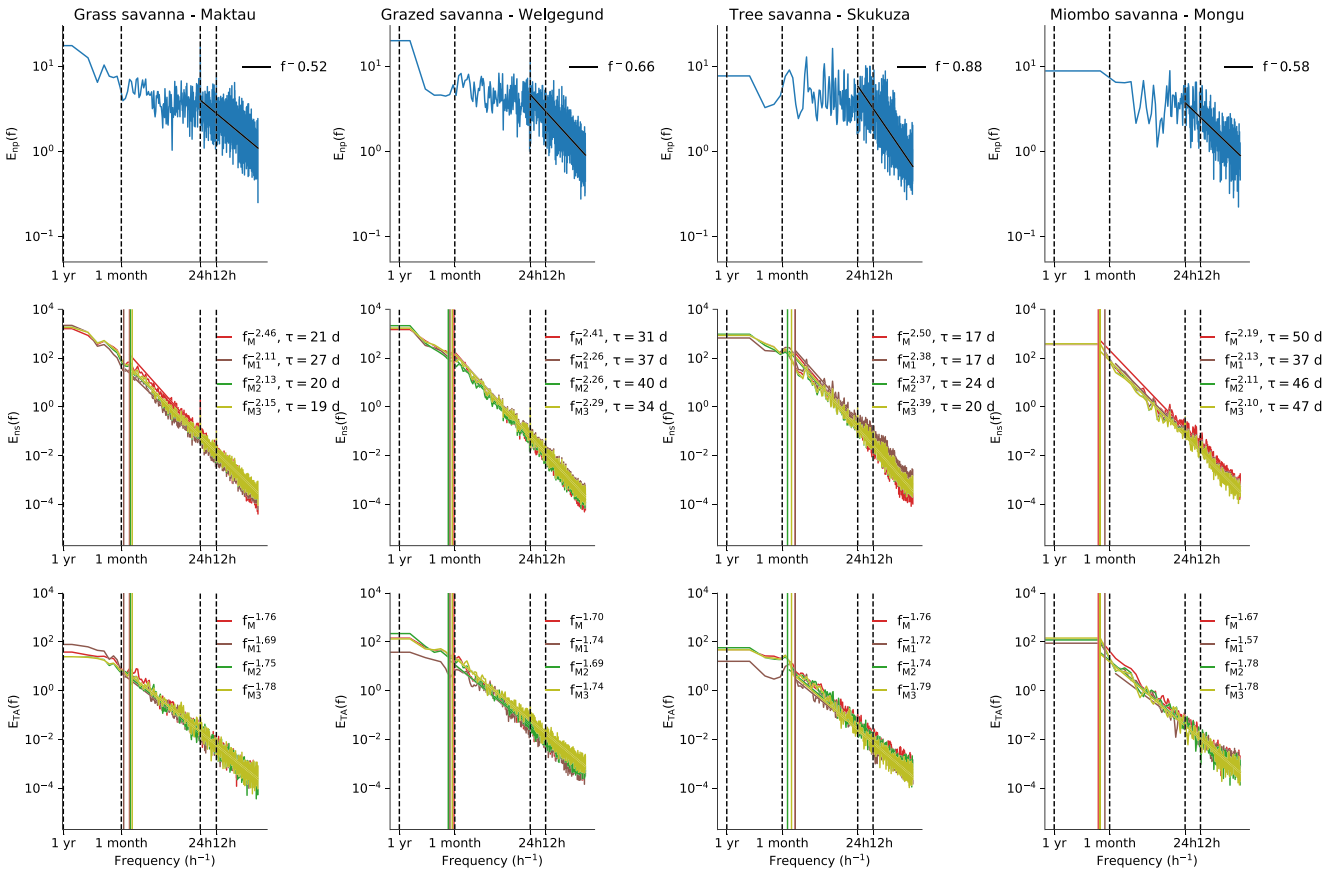

FIGURE 7 Normalized spectrum of measured precipitation ($E_{np}(f)$), measured and modelled soil moisture ($E_{ns}(f)$) and its telegraphic approximation (ETA(f)) for the four savanna sites. The red, brown, green and yellow colours show the measured, Model 1, Model 2 and Model 3 results, respectively. The memory timescales (τ) are indicated with solid vertical lines with corresponding colour. The black dashed vertical lines indicate diurnal (12 h), daily (24 h), monthly and yearly time periods

persistence fit parameter β were not directly related as evidenced by the similar β at grass and miombo savannas. The β parameter describes to which degree the dry periods are power law distributed (lower β) or exponentially decaying at long times (higher β).

The long dry periods in the grass savanna soil moisture series (Figure 4) are clearly clustered at the tail of the dry persistence (Figure 9). The dry persistence parameter β was higher at grazed and tree savannas and lower at the grass and miombo savanna sites. This means that the longest dry periods at the grass site are due to wet seasons at which the soil moisture never crosses the water-stress threshold to a wet state (Figure 4). In contrast, at the miombo savanna during wet season, dry periods are short. This pattern leads to many short dry periods and one long dry period per year. For these reasons, the grass and miombo sites have lower β, which means that the dry persistence is closer to power law (i.e. heavy-tailed). Despite the drought occurrence, the grazed and tree savannas did not experience a wet season in which soil moisture would persist at low values at all times, and thus, the dry persistence has more exponential decay at long times.

The differences between model and measured β can be explained by the differences of the modelled and measured soil moisture near the s^* crossings (Figure 4). As noted earlier, the agreement between Model 3 and s measurements was similar near s^* crossings at the grass and tree savannas. This agreement also resulted in a β value that is close to the measured value. All models underestimate soil moisture near s^* at the grazed site, and thus, the modelled β values are lower than the measured β. The miombo savanna soil moisture series were only 1 year long, and this short record is expected to lead to fewer dry periods and a large mismatch between the fitted lines and the bins.

The mean annual dry period ($\bar{T}_*$) was estimated for the full hydrological years at the grass, grazed and tree savanna sites (Table 3). The predicted $\bar{T}_*$ by Models 2 and 3 is closer to the measured $\bar{T}_*$, and their standard deviation is smaller. The large difference between Models 1 and 3 estimates at the grazed savanna is explained by the difference in annual mean periods between models during the drought years. Model 1 does not take into account the reduction in E_{max} during the drought years. This lack of reduction in E_{max} by Model 1 results in much longer mean dry periods during drought years. The large

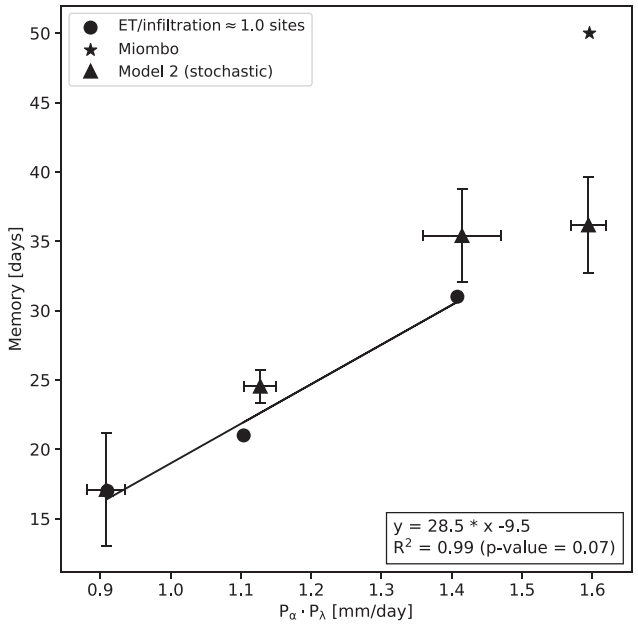

FIGURE 8 The relation between daily mean rainfall intensity, $P_\alpha \cdot P_\lambda$, and the soil moisture memory timescale. The dots indicate measured value for the three sites with evapotranspiration(ET)/infiltration ∼ 1.0, and the star indicates measured values at miombo. The triangles indicate mean values and error bars indicate ±1 standard deviation from 50 stochastic simulations

underestimation of Model 1 $\bar{T}_*$ at the grass savanna is due to the years 2014 to 2015 (Figure 4) when Model 1 has s^* crossing. For this period, the tree savanna storm frequency was 0.17, which is 0.05 lower than at the grazed savanna.

3.4 | Sensitivity of Model 3 memory and dry persistence

A sensitivity analysis of Model 3 reveals that the modelled memory increases linearly with increasing s_* and s_{fc}, but memory does not vary owing to changes in MAP (Figure 10). The modelled memory is most sensitive to the changes in soil moisture thresholds at the tree savanna that had the lowest s^*.

For all the sites, Model 3 dry persistence parameter β increases with increasing MAP. The higher precipitation results in shorter maximum dry periods that then lead to more exponential decay of the long dry periods. The modelled β at the grass savanna site is less sensitive to changes in MAP than at the grazed and tree savannas. The β changes at miombo savanna should be considered uncertain owing to the short record.

4 | DISCUSSION

The hierarchy of models shows that Model 1 with only rainfall variability captures a large part of the soil moisture spectral decay. Moreover, the work here demonstrated that including NDVI and PET does not introduce significant energy (or activity) additions to seasonal timescales in the soil moisture spectrum. However, accounting for NDVI and PET variability does improve model fit by adjusting the maximum ET loss and accounting for interannual variation in ET. This improvement is needed for correct memory and dry persistence estimation. Similarly, previous ecohydrological model study highlighted interannual variation in transpiration that is also captured here through NDVI variability (Miller et al., 2012). Linear relation between soil moisture memory and precipitation intensity was observed in measurements and in stochastic simulations across three savannas with ET/infiltration ∼ 1.0. The differences in the timing and length of dry periods between the savannas reveal new aspects relevant to stochastic soil moisture models regarding the seasonality of the forcing.

The memory timescale is primarily controlled by the losses, not the precipitation statistics. For an idealized system where white-noise precipitation is the main forcing and a linear ET-soil moisture loss function represents the large losses from the system, the memory can be predicted analytically to be $(\eta Z_r)/E_{max}$ (Nakai et al., 2014). This means that the size of the water reservoir ($=\eta Z_r$) and the maximum loss rate (= E_{max}) are responsible for setting the memory timescales. The measured precipitation intensity and memory timescale were linearly related across three savannas that were dominated by ET losses. This does not mean that memory is controlled by the forcing but instead there is a link between rainfall statistics and maximum ET. When ET/infiltration ∼ 1.0, then the losses are dominated by ET (at sufficiently long timescale), and it equals the mean rainfall intensity adjusted by interception loss (eq. 2.46, Rodríguez-Iturbe & Porporato, 2007). This relation was also shown with stochastic Poisson precipitation that includes dry seasons using the model with NDVI variability on maximum ET. For measured precipitation and memory, the difference in root-zone length most likely explains the slightly higher memory than expected from precipitation intensity on the grazed savanna. This relation is most relevant for shallow-rooted savannas that receive rainfall around or less than 500 mm because the losses are often dominated by ET (Miller et al., 2012; Scott & Biederman, 2019). The 30-cm root-zone depth is estimated to contain 57% of the root biomass for tropical grassland savannas (Jackson et al., 1996). For four African savannas (P = 294–661 mm), the ET/P ratio ranged from 87% to 94% (Miller et al., 2012), which is a similar range at the three savanna sites here. Model 1 simulation for the lowest rainfall frequency site shows that the overestimation of dry periods may lead to correct memory estimation despite overestimated ET losses due to increased minimum soil moisture periods. The analysis at this spatial and temporal scales suggests that in the latitude range (from 3 to 26) of the savanna sites, the measured memory timescale does not scale with latitude in the way it scales for a seminal climate model analysis from subtropical to midlatitude (Delworth & Manabe, 1988).

The distribution of times when soil moisture was below the plant water-stress threshold revealed that the savannas can have

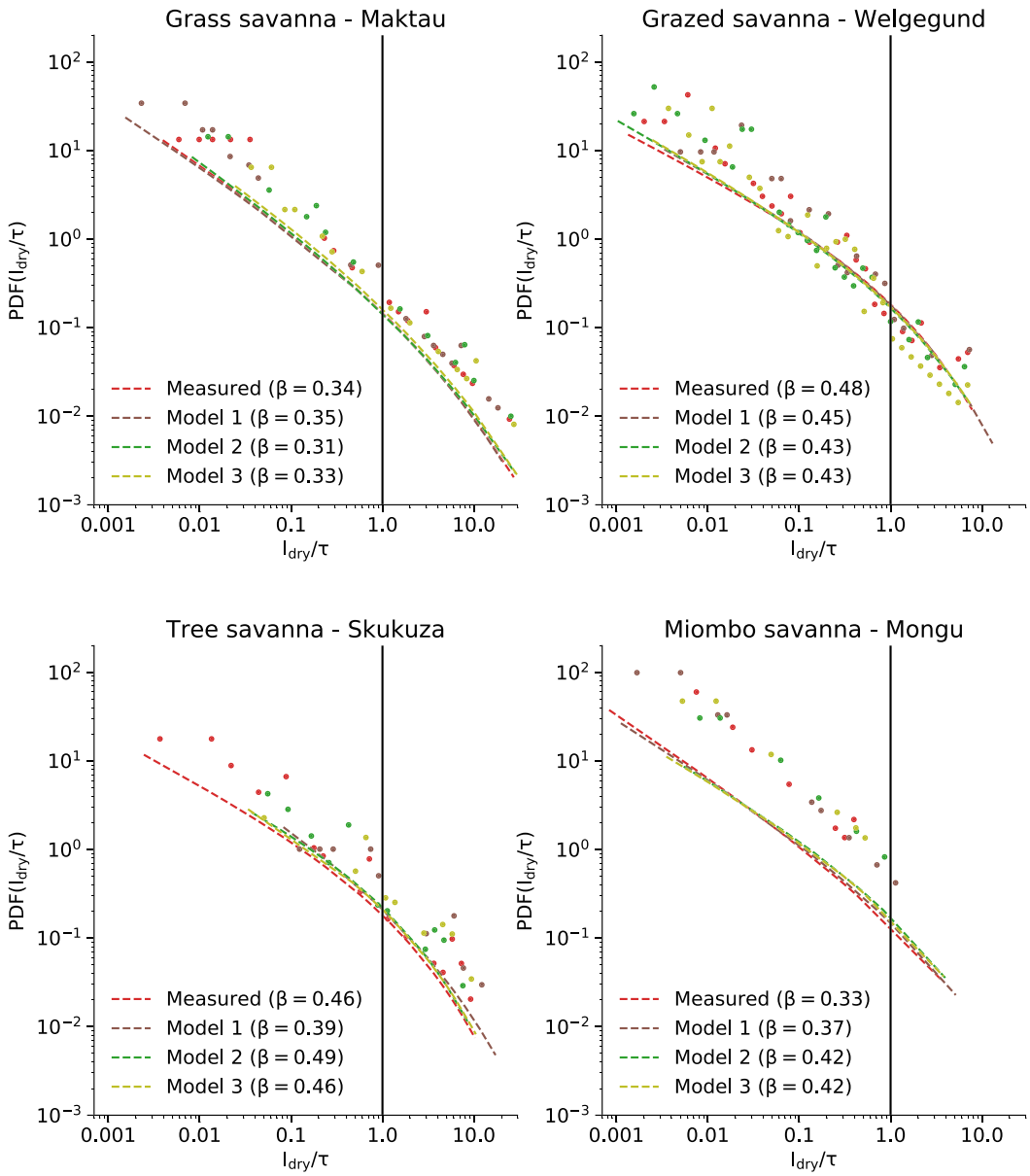

FIGURE 9 The probability density function (PDF) of persistence times of soil moisture below s^* divided by the site-specific memory timescale. The red, brown, green and yellow lines indicate the fit to the Equation 12 for the measured, Model 1, Model 2 and Model 3 results. The dots indicate logarithmically spaced bins. The vertical lines indicate the memory timescales determined at 21, 31, 17 and 50 days for the grass, grazed, tree and miombo savannas, respectively

TABLE 3 Model estimate of mean annual dry period ($\bar{T}_*$) and standard deviation for grass, grazed and tree savannas

Site	Measured $\bar{T}_*$	Model 1 $\bar{T}_*$	Model 2 $\bar{T}_*$	Model 3 $\bar{T}_*$
Grass	170 ± 30	130 ± 40	180 ± 40	170 ± 30
Grazed	40 ± 60	80 ± 80	40 ± 50	30 ± 40
Tree	-	60 ± 80	50 ± 50	50 ± 40

Note: Estimated from at least four full hydrological years. Measured soil moisture was not available for tree savanna.

either closer to power law or exponential decay at long times. Model 3 was able to distinguish the lower β values that indicate power-law scaling and higher β values that indicate exponential decay. The measured mean annual dry periods ($\bar{T}_*$) agreed with the differences in β at grass and grazed savannas. In general, the use of dry persistence is more difficult than memory because of lack of theoretical results. However, more detailed differences in long dry periods at each site can be discussed based on the time series of soil moisture (Figure 4). The Kenyan grass savanna site shows high inter-annual variability between the timing of short and long rainy seasons, and the dry persistence parameter may enable to distinguish the years with short and long separation between the two rainy seasons. A method to separate dry and wet seasons is important if the Poisson rainfall is used as forcing. This rainfall timing variability also suggests

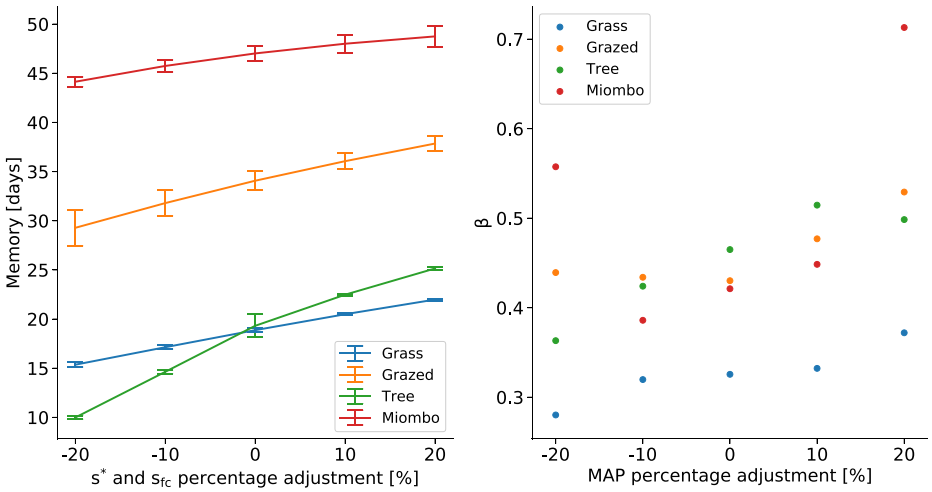

FIGURE 10 Model 3 memory sensitivity to changes in s^* and sfc and Model 3 dry persistence parameter sensitivity to changes in mean annual precipitation (MAP). The error bars indicate ±1 standard deviation of the memory due to differences in MAP

that continuous seasonality forcing (Feng, Porporato, & Rodriguez-Iturbe, 2015) represented here by observed NDVI rather than ad hoc seasonally 'averaged' forcing may be more appropriate method to account for seasonality in the analytical framework for the bimodal rainfall site. Alternatively, a suite of methods that define the start of the dry season could be tested as was done at a site in a Mediterranean climate (Dralle & Thompson, 2016). These methods could be used to quantify the carry-over moisture from short to long rains and the mean soil moisture in stochastic steady state. The drought year in grazed savanna shows that in-season dry spell can be comparable with the dry season length. At this site, the PET variability is also important. The miombo savanna is the only site with the tail of dry persistence defined by the long dry season. This was confirmed from 100-year monthly rainfall series showing that considerable dry season precipitation and in-season dry spells are rare.

The model fit was sensitive to the values of s^* and s_{fc}. The eddy covariance-derived s^* resulted in an acceptable model fit compared with measured soil moisture. Moreover, the estimated s^* values agree with the species specific trend that grass species have higher s^* than tree species (Rodríguez-Iturbe & Porporato, 2007) shown here by the 0.1 higher s^* on the grazed savanna that has half the tree cover of the tree savanna. The estimated $E_{max,EC}$ was 3.3 and 3.4 mm/day for the South African grazed and tree savannas, respectively. These values are lower than the grass (E_{max} = 5.0 mm/day) value estimated for the Nylsvley savanna in South Africa (Rodríguez-Iturbe & Porporato, 2007). The ad hoc rule $s_{fc} = s^*/0.75$ resulted in lower s_{fc} than a soil texture-based value reported by Laio, Porporato, Ridolfi and Rodriguez-Iturbe (2001). This estimate gives also comparable or lower grass layer s_{fc} values than estimated values for four African savannas reported by Miller et al. (2012). The resulting drainage was low in all three models for three sites, and thus, much higher s_{fc} may not be justified. This method to estimate s^* and maximum ET offers an alternative to the water retention curve-based s^* and Priestley–Taylor estimated maximum ET (Miller et al., 2007).

5 | MODEL AND DATA LIMITATIONS

5.1 | Model limitations

The lumped hydrological balance employed in Models 1–3 makes a number of assumptions about lateral flow, ponding and reinfiltration; links between bulk root-zone soil moisture and water losses from the rooting zone; and water inputs into the rooting zone. Most restrictive is that the approach further assumes that the rooting zone depth is constant throughout the study period. The modelled soil moisture had the largest deviations from measured soil moisture when interception loss was different from the estimated mean loss or when drainage was significant. This approach does not consider the precipitation event structure or non-linear changes in interception loss due to storm characteristics. The miombo savanna had a lower mean interception during early wet season and considerable drainage during the wet season, which was underestimated by the models despite high K_{sat} and parameter c. For these reasons, the proposed approach at hourly timescale here is better suited to dry savannas (MAP < 600 mm), where ET losses dominate.

5.2 | Data limitations

The use of measurements that sample different scales and locations also poses challenges above and beyond sensor precision. The soil moisture measurements are sampled at small scales as compared with the eddy-covariance measurements and the processes represented by the hydrological model. Also, the precipitation measurements themselves need not represent events at the location, where soil moisture is measured. Moreover, the spatial variability of soil moisture is known to be large even at small scales (Katul, Todd, Pataki, Kabala, & Oren, 1997), which makes comparisons between modelled and absolute soil moisture difficult. This difficulty is compounded by the fact that the root-zone vertically averaged soil moisture is measured using multiple probes, each assumed to represent different layers. Horizontally, there

are clear differences in soil moisture time traces (and associated soil moisture memory) between open and closed canopy locations. Interestingly, variability in soil moisture may be better captured by the soil moisture measurements as apparent in the superior agreement between measured and modelled spectra, even when the time traces of modelled soil moisture exhibit some biases.

Last, the duration of the record here may be short to sample an ensemble of climatic extremes. The 1-year-long time series at miombo savanna were simply too short to differentiate NDVI only and NDVI-PET model differences. There could also be energy-related changes in soil moisture spectra at seasonal scales that simply cannot be estimated here but have been observed at forested sites (Nakai et al., 2014). The grazed savanna had a long enough time series for which the PET-NDVI improved the model fit. The NDVI variability was presumed to represent LAI changes, and its effect on ET was through parameter a_2. The grass and grazed savannas have a tree cover of less than 15%, and thus, the NDVI is expected to represent the grass leaf area dynamics. The increase of ET loss from the drought year to normal year was evident in measured soil moisture series at the tree savanna, and thus, the trend in NDVI reflects the grass layer dynamics despite the 30% tree cover.

6 | CONCLUSIONS

Through hierarchy of approximations applied to a lumped water balance model and analysis of measured soil moisture, it was demonstrated that precipitation variability alone explains much of the soil moisture variance at high frequencies (hourly to days). However, adjustments to maximum ET with NDVI and PET variability improved the model fit to measured soil moisture and concomitant memory timescale estimates. This improvement is of significance when dry persistence and mean annual dry periods are to be estimated from lumped models widely used in climate and ecohydrological sciences. For ET-dominated savannas, precipitation intensity and memory were linearly related across sites. This is an interesting finding that should be included as a new summary in future stochastic models of savannas. It may be used to explore contrasting precipitation seasonality without separating the analysis between dry and wet seasons. The intensity–memory relation might be different at sites with highly seasonal precipitation because long dry periods decrease precipitation intensity, and drainage may become a far more significant contributor to the loss term in the hydrological balance. Also, highly seasonal precipitation may support only conservative water use that leads to longer memory timescales. Thus, the seasonality of the forcing and the differences in the timing of long dry periods at the sites have important implications for the stochastic steady-state analysis of mean soil moisture.

ACKNOWLEDGEMENTS

This study was supported by the Academy of Finland through the projects TAITAWATER (grant number 261280)—Integrated land cover–climate–ecosystem process study for water management in East African highlands and SMARTLAND (grant number 318645)—Environmental sensing of ecosystem services for developing climate smart landscape to improve food security in East Africa (PI P. Pellikka). The Taita Research Station of University of Helsinki is acknowledged for logistical support and M. Mjomba for the help during the field campaigns in Kenya. Funding for the operation of the Skukuza flux tower site for the period of data used was obtained from the Council for Scientific and Industrial Research Parliamentary Grant under the South African Integrated Carbon Observation Network project and from the ARS AfricaE (Adaptive Resilience of Southern African Ecosystems) project funded under the SPACES Programme (Science Partnerships for the Assessment of Complex Earth System Processes) of the Bundesministerium für Bildung und Forschung (German Federal Ministry of Education and Research) (grant number 01LL1303). This work was partially funded by the European Commission through the project 'Supporting EU-African Cooperation on Research Infrastructures for Food Security and Greenhouse Gas Observations' (SEACRIFOG; project ID 730995). This publication forms part of the output of the Biogeochemistry Research Infrastructure Platform (BIOGRIP) of the Department of Science and Innovation of South Africa. G. Katul acknowledges partial support from the U.S. National Science Foundation (NSF-AGS-1644382 and NSF-IOS-1754893). The data used in this study are available online https://doi.org/10.6084/m9.figshare.11310659 (Räsänen et al., 2019).

ORCID

Matti Räsänen https://orcid.org/0000-0003-0994-5353

REFERENCES

AghaKouchak, A. (2015). A multivariate approach for persistence-based drought prediction: Application to the 20,102,011 East Africa drought. *Journal of Hydrology*, *526*, 127–135. https://doi.org/10.1016/j.jhydrol.2014.09.063

Al-Kaisi, M., Brun, L. J., & Enz, J. W. (1989). Transpiration and evapotranspiration from maize as related to leaf area index. *Agricultural and Forest Meteorology*, *48*(1), 111–116. https://doi.org/10.1016/0168-1923(89)90010-5

Archibald, S. A., Kirton, A., van der Merwe, M. R., Scholes, R. J., Williams, C. A., & Hanan, N. (2009). Drivers of inter-annual variability in Net Ecosystem Exchange in a semi-arid savanna ecosystem, South Africa. *Biogeosciences*, *6*(2), 251–266. https://doi.org/10.5194/bg-6-251-2009

Cava, D., & Katul, G. G. (2009). The effects of thermal stratification on clustering properties of canopy turbulence. *Boundary-Layer Meteorology*, *130*(3), 307–325. https://doi.org/10.1007/s10546-008-9342-6

Cava, D., Katul, G. G., Molini, A., & Elefante, C. (2012). The role of surface characteristics on intermittency and zero-crossing properties of atmospheric turbulence: Clustering in atmospheric turbulence. *Journal of Geophysical Research-Atmospheres*, *117*(D1), n/a–n/a. https://doi.org/10.1029/2011JD016167

Delworth, T. L., & Manabe, S. (1988). The influence of potential evaporation on the variabilities of simulated soil wetness and climate. *Journal of Climate*, *1*(5), 523–547. https://doi.org/10.1175/1520-0442(1988)001<0523:TIOPEO>2.0.CO;2

Didan, K. (2015). MOD13Q1 MODIS/Terra Vegetation Indices 16-Day L3 Global 250 m SIN Grid V006, NASA EOSDIS Land Processes DAAC. 10.5067/MODIS/MOD13Q1.006.

Dralle, D. N., & Thompson, S. E. (2016). A minimal probabilistic model for soil moisture in seasonally dry climates: Seasonal soil moisture PDFs. *Water Resources Research*, *52*(2), 1,507–1,517. https://doi.org/10.1002/2015WR017813

Feng, X., Porporato, A., & Rodriguez-Iturbe, I. (2015). Stochastic soil water balance under seasonal climates. *Proc. R. Soc. A*, *471*(2174), 1–17. https://doi.org/10.1098/rspa.2014.0623

Ghannam, K., Nakai, T., Paschalis, A., Oishi, C. A., Kotani, A., Igarashi, Y., … Katul, G. G. (2016). Persistence and memory timescales in root-zone soil moisture dynamics. *Water Resources Research*, *52*(2), 1,427–1,445. https://doi.org/10.1002/2015WR017983

Green, J. K., Konings, A. G., Alemohammad, S. H., Berry, J., Entekhabi, D., Kolassa, J., … Gentine, P. (2017). Regionally strong feedbacks between the atmosphere and terrestrial biosphere. *Nature Geoscience*, *10*(6), 410–414. https://doi.org/10.1038/ngeo2957

Isaac, P., Cleverly, J., McHugh, I., van Gorsel, E., Ewenz, C., & Beringer, J. (2017). OzFlux data: Network integration from collection to curation. *Biogeosciences*, *14*(12), 2,903–2,928.

Jaars, K., Beukes, J. P., van Zyl, P. G., Venter, A. D., Josipovic, M., Pienaar, J. J., … Hakola, H. (2014). Ambient aromatic hydrocarbon measurements at Welgegund, South Africa. *Atmospheric Chemistry and Physics*, *14*(13), 7,075–7,089. https://doi.org/10.5194/acp-14-7075-2014

Jaars, K., van Zyl, P. G., Beukes, J. P., Hellén, H., Vakkari, V., Josipovic, M., … Hakola, H. (2016). Measurements of biogenic volatile organic compounds at a grazed savannah grassland agricultural landscape in South Africa. *Atmospheric Chemistry and Physics*, *16*(24), 15,665–15,688. https://doi.org/10.5194/acp-16-15665-2016

Jaars, K., Vestenius, M., van Zyl, P. G., Beukes, J. P., Hellén, H., Vakkari, V., … Hakola, H. (2018). Receptor modelling and risk assessment of volatile organic compounds measured at a regional background site in South Africa. *Atmospheric Environment*, *172*, 133–148. https://doi.org/10.1016/j.atmosenv.2017.10.047

Jackson, R. B., Canadell, J., Ehleringer, J. R., Mooney, H. A., Sala, O. E., & Schulze, E. D. (1996). A global analysis of root distributions for terrestrial biomes. *Oecologia*, *108*(3), 389–411.

Katul, G. G., Porporato, A., Daly, E., Oishi, A. C., Kim, H.-S., Stoy, P. C., … Siqueira, M. B. (2007). On the spectrum of soil moisture from hourly to interannual scales. *Water Resources Research*, *43*(5), 1–10. https://doi.org/10.1029/2006WR005356

Katul, G. G., Wendroth, O. B., Parlange, M. B., Puente, C. E., & Nielsen, D. R. (1993). Estimation of in situ hydraulic conductivity function from nonlinear filtering theory. *Water Resources Research*, *29*, 1,063–1,070.

Katul, G., Todd, P., Pataki, D., Kabala, Z. J., & Oren, R. (1997). Soil water depletion by oak trees and the influence of root water uptake on the moisture content spatial statistics. *Water Resources Research*, *33*(4), 611–623.

Koster, R. D., Dirmeyer, P. A., Guo, Z., Bonan, G., Chan, E., Cox, P., … Yamada, T. (2004). Regions of strong coupling between soil moisture and precipitation. *Science*, *305*(5687), 1,138–1,140. https://doi.org/10.1126/science.1100217

Kulmatiski, A., & Beard, K. H. (2013). Root niche partitioning among grasses, saplings, and trees measured using a tracer technique. *Oecologia*, *171*(1), 25–37. https://doi.org/10.1007/s00442-012-2390-0

Kutsch, W. L., Merbold, L., Ziegler, W., Mukelabai, M. M., Muchinda, M., Kolle, O., & Scholes, R. J. (2011). The charcoal trap: Miombo forests and the energy needs of people. *Carbon Balance and Management*, *6*(1), 1–11.

Laherrère, J., & Sornette, D. (1998). Stretched exponential distributions in nature and economy: "Fat tails" with characteristic scales. *The European Physical Journal B*, *2*(4), 525–539. https://doi.org/10.1007/s100510050276

Laio, F., Porporato, A., Ridolfi, L., & Rodriguez-Iturbe, I. (2001). Plants in water-controlled ecosystems: Active role in hydrologic processes and response to water stress. *Advances in Water Resources*, *24*(7), 707–723. https://doi.org/10.1016/S0309-1708(01)00005-7

Laio, F., Porporato, A., Fernandez-Illescas, C. P., & Rodriguez-Iturbe, I. (2001). Plants in water-controlled ecosystems: Active role in hydrologic processes and response to water stress: IV. *Discussion of real cases, Advances in Water Resources*, *24*(7), 745–762. https://doi.org/10.1016/S0309-1708(01)00007-0

Lorenz, R., Jaeger, E. B., & Seneviratne, S. (2010). Persistence of heat waves and its link to soil moisture memory. *Geophysical Research Letters*, *37*(9), 1–5. https://doi.org/10.1029/2010GL042764

Masih, I., Maskey, S., Mussá, F. E. F., & Trambauer, P. (2014). A review of droughts on the African continent: A geospatial and long-term perspective. *Hydrology and Earth System Sciences*, *18*(9), 3,635–3,649. https://doi.org/10.5194/hess-18-3635-2014

Miller, G. R., Baldocchi, D. D., Law, B. E., & Meyers, T. (2007). An analysis of soil moisture dynamics using multi-year data from a network of micrometeorological observation sites. *Advances in Water Resources*, *30*(5), 1,065–1,081. https://doi.org/10.1016/j.advwatres.2006.10.002

Miller, G. R., Cable, J. M., McDonald, A. K., Bond, B., Franz, T. E., Wang, L., … Scott, R. L. (2012). Understanding ecohydrological connectivity in savannas: A system dynamics modelling approach. *Ecohydrology*, *5*(2), 200–220. https://doi.org/10.1002/eco.245

Molini, A., Katul, G. G., & Porporato, A. (2009). Revisiting rainfall clustering and intermittency across different climatic regimes. *Water Resources Research*, *45*(11), 1–13. https://doi.org/10.1029/2008WR007352

Moon, H., Gudmundsson, L., & Seneviratne, S. I. (2018). Drought persistence errors in global climate models. *Journal of Geophysical Research-Atmospheres*, *123*(7), 3,483–3,496. https://doi.org/10.1002/2017JD027577

Nakai, T., Katul, G. G., Kotani, A., Igarashi, Y., Ohta, T., Suzuki, M., & Kumagai, T. (2014). Radiative and precipitation controls on root zone soil moisture spectra. *Geophysical Research Letters*, *41*(21), 7,546–7,554. https://doi.org/10.1002/2014GL061745

Parlange, M. B., Katul, G. G., Cuenca, R. H., Kavvas, M. L., Nielsen, D. R., & Mata, M. (1992). Physical basis for a time series model of soil water content. *Water Resources Research*, *28*(9), 2,437–2,446.

Pastorello, G., Papale, D., Chu, H., Trotta, C., Agarwal, D., Canfora, E., … Torn, M. (2017). The fluxnet2015 dataset: The longest record of global carbon, water, and energy fluxes is updated. *Eos*, *98*.

Pumo, D., Viola, F., & Noto, L. V. (2008). Ecohydrology in Mediterranean areas: A numerical model to describe growing seasons out of phase with precipitations. *Hydrology and Earth System Sciences*, *12*(1), 303–316. https://doi.org/10.5194/hess-12-303-2008

Porporato, A., Laio, F., Ridolfi, L., & Rodriguez-Iturbe, I. (2001). Plants in water-controlled ecosystems: Active role in hydrologic processes and response to water stress: III. *Vegetation water stress, Advances in Water Resources*, *24*(7), 725–744. https://doi.org/10.1016/S0309-1708(01)00006-9

Porporato, A., Daly, E., & Rodriguez-Iturbe, I. (2004). Soil water balance and ecosystem response to climate change. *The American Naturalist*, *164*(5), 625–632. https://doi.org/10.1086/424970

Priestley, C. H. B., & Taylor, R. (1972). On the assessment of surface heat flux and evaporation using large-scale parameters. *Monthly Weather Review*, *100*(2), 81–92.

Priestley, M. B. (1981). *Spectral analysis and time series*. London: Academic Press.

Räsänen, M., Aurela, M., Vakkari, V., Beukes, J. P., Tuovinen, J.-P., Van Zyl, P. G., … Laakso, L. (2017). Carbon balance of a grazed savanna grassland ecosystem in South Africa. *Biogeosciences*, *14*(5), 1,039–1,054. https://doi.org/10.5194/bg-14-1039-2017

Räsänen, M., Merbold, L., Vakkari, V., Aurela, M., Laakso, L., Beukes, P., … Katul, G. G. (2019). Dataset for "Root-zone soil moisture variability

across African savannas: From pulsed rainfall to landcover switches". https://doi.org/10.6084/m9.figshare.11310659.v1

Reichstein, M., Falge, E., Baldocchi, D., Papale, D., Aubinet, M., Berbigier, P., … Valentini, R. (2005). On the separation of net ecosystem exchange into assimilation and ecosystem respiration: Review and improved algorithm. *Global Change Biology*, *11*(9), 1,424–1,439. https://doi.org/10.1111/j.1365-2486.2005.001002.x

Rigden, A. J., & Salvucci, G. D. (2017). Stomatal response to humidity and CO_2 implicated in recent decline in US evaporation. *Global Change Biology*, *23*(3), 1,140–1,151. https://doi.org/10.1111/gcb.13439

Rodriguez-Iturbe, I., Porporato, A., Ridolfi, L., Isham, V., & Coxi, D. R. (1999). Probabilistic modelling of water balance at a point: The role of climate, soil and vegetation. *Proceedings of the Royal Society A: Mathematical, Physical and Engineering Sciences*, *455*(1990), 3,789–3,805. https://doi.org/10.1098/rspa.1999.0477

Rodríguez-Iturbe, I., & Porporato, A. (2007). *Ecohydrology of water-controlled ecosystems: Soil moisture and plant dynamics*. Cambridge, UK: Cambridge University Press.

Saini, R., Wang, G., & Pal, J. S. (2016). Role of soil moisture feedback in the development of extreme summer drought and flood in the United States. *Journal of Hydrometeorology; Boston*, *17*(8), 2,191–2,207. https://doi.org/10.1175/JHM-D-15-0168.1

Scholes, R. J., Gureja, N., Giannecchinni, M., Dovie, D., Wilson, B., Davidson, N., … Ndala, S. (2001). The environment and vegetation of the flux measurement site near Skukuza, Kruger National Park. *Koedoe*, *44*(1), 73–83. https://doi.org/10.4102/koedoe.v44i1.187

Schwinning, S., & Sala, O. E. (2004). Hierarchy of responses to resource pulses in arid and semi-arid ecosystems. *Oecologia*, *141*(2), 211–220. https://doi.org/10.1007/s00442-004-1520-8

Scott, R. L., & Biederman, J. A. (2019). Critical zone water balance over 13 years in a semiarid savanna. *Water Resources Research*, *55*(1), 574–588. https://doi.org/10.1029/2018WR023477

Siqueira, M., Katul, G., & Porporato, A. (2009). Soil moisture feedbacks on convection triggers: The role of soil–plant hydrodynamics. *Journal of Hydrometeorology*, *10*(1), 96–112.

Sreenivasan, K. R., & Bershadskii, A. (2006). Clustering properties in turbulent signals. *Journal of Statistical Physics*, *125*(5–6), 1,141–1,153. https://doi.org/10.1007/s10955-006-9112-0

Taylor, C. M., Gounou, A., Guichard, F., Harris, P. P., Ellis, R. J., Couvreux, F., & Kauwe, M. D. (2011). Frequency of Sahelian storm initiation enhanced over mesoscale soil-moisture patterns. *Nature Geoscience*, *4*(7), 430–433. https://doi.org/10.1038/ngeo1173

Teuling, A. J. (2005). On bimodality in warm season soil moisture observations. *Geophysical Research Letters*, *32*(13), 1–4. https://doi.org/10.1029/2005GL023223

Wang, L., D'Odorico, P., Ringrose, S., Coetzee, S., & Macko, S. A. (2007). Biogeochemistry of Kalahari sands. *Journal of Arid Environments*, *71*(3), 259–279. https://doi.org/10.1016/j.jaridenv.2007.03.016

Wei, J., Dickinson, R. E., & Chen, H. (2008). A negative soil moisture–precipitation relationship and its causes. *Journal of Hydrometeorology*, *9*(6), 1,364–1,376.

Welch, P. (1967). The use of fast Fourier transform for the estimation of power spectra: A method based on time averaging over short, modified periodograms. *IEEE Transactions on Audio and Electroacoustics*, *15*(2), 70–73. https://doi.org/10.1109/TAU.1967.1161901

Whitley, R., Beringer, J., Hutley, L. B., Abramowitz, G., Kauwe, M. G. D., Duursma, R., … Yu, Q. (2016). A model inter-comparison study to examine limiting factors in modelling Australian tropical savannas. *Biogeosciences*, *13*(11), 3,245–3,265. https://doi.org/10.5194/bg-13-3,245-2016

Whitley, R., Beringer, J., Hutley, L. B., Abramowitz, G., Kauwe, M. G. D., Evans, B., … Yu, Q. (2017). Challenges and opportunities in land surface modelling of savanna ecosystems. *Biogeosciences*, *14*(20), 4,711–4,732. https://doi.org/10.5194/bg-14-4,711-2017

Williams, C. A., & Albertson, J. D. (2004). Soil moisture controls on canopy-scale water and carbon fluxes in an African savanna. *Water Resources Research*, *40*(9), 1–14. https://doi.org/10.1029/2004WR003208

Yin, J., Porporato, A., & Albertson, J. (2014). Interplay of climate seasonality and soil moisture-rainfall feedback. *Water Resources Research*, *50*(7), 6,053–6,066. https://doi.org/10.1002/2013WR014772

SUPPORTING INFORMATION

Additional supporting information may be found online in the Supporting Information section at the end of this article.

How to cite this article: Räsänen M, Merbold L, Vakkari V, et al. Root-zone soil moisture variability across African savannas: From pulsed rainfall to land-cover switches. *Ecohydrology*. 2020;e2213. https://doi.org/10.1002/eco.2213